EHLCATHOL

D6.1 Bibliographical study on EHL-derived fuel combustion properties – Revised version

Ismahane Meziane, Nicolas Delort, Olivier Herbinet, Frédérique Battin-Leclerc, Yongdan Li, Saravanan Kasipandi

EHLCATHOL – http://ehlcathol.eu/

This project has received funding from the European Union's Horizon 2020 research and innovation programme under grant agreement No 101006744

Grant Agreement Number	101006744
Action Acronym	EHLCATHOL
Action Title	Chemical Transformation of Enzymatic Hydrolysis Lignin (EHL) with Catalytic Solvolysis to Fuel Commodities Under Mild Conditions (EHLCATHOL)
Funding Scheme	H2020-LC-SC3-2020-RES-RIA
Version date of Grant Agreement against which the assessment will be made	27/10/2020
Start date of the project	01/11/2020
Due date of the deliverable	31/10/2021
Actual date of submission	29/10/2021, Date of resubmission: 14/12/2021
Responsible	CNRS
Contributors	Aalto University
Dissemination level	Public

This document has been produced by the EHLCATHOL project, funded by the Horizon 2020 Programme of the European Community. The content presented in this document represents the views of the authors, and the European Commission has no liability in respect of the content.

Authors in alphabetical order

Full Name	Organization	E-mail
Frederique Battin-Leclerc	CNRS	frederique.battin-leclerc@univ-lorraine.fr
Nicolas Delort	CNRS	nicolas.delort@univ-lorraine.fr
Olivier Herbinet	CNRS	olivier.herbinet@univ-lorraine.fr
Saravanan Kasipandi	Aalto University	saravanan.saravanankasipandi@aalto.fi
Yongdan Li	Aalto University	yongdan.li@aalto.fi
Ismahane Meziane	CNRS	ismahane.meziane@univ-lorraine.fr

Change History

Version	Date	Status	Author (Company)	Description
1.0	29/10/2021	Submitted	Frédérique Battin-Leclerc	Original, submitted version
1.1	29/11/2021	Revised version	Frédérique Battin-Leclerc	P. 5: the 2nd paragraph was completed; p. 30-39: a new part 4 was added: "4. Description of the literature studies concerning the combustion kinetics of oxygenated aromatics, which are the main components of EHL-derived fuels" and includes 8 tables; P. 40: the 3rd paragraph was added.

TABLES OF CONTENTS

Notations **4**

Summary **5**

1. Introduction **6**

1.1. Cellulose 6

1.2. Hemicellulose 6

1.3. Lignin 7

1.4. Enzymatic hydrolysis lignin 9

2. Bibliographic review of experimental studies on the valorization of lignin and EHL to the production of bio-oils. **12**

2.1. Lignin valorization to biofuels 12

2.2. Enzymatic hydrolysis lignin valorization to biofuels 19

3. Bibliographical study on EHL-derived fuels and their combustion properties **24**

4. Description of the literature studies concerning the combustion kinetics of oxygenated aromatics, which are the main components of EHL-derived fuels **29**

4.1. Phenol 30

4.2. Anisole 31

4.3. Benzyl alcohol 32

4.4. Phenyl-ethanols 33

4.5. Catechol 34

4.6. Cresols 35

4.7. Guaiacol 35

4.8. Summary of species produced during the oxidation of oxygenated aromatics 36

4.9. Conclusion for this part 38

5. Conclusion **39**

References **40**

Notations

EHL	**Enzymatic Hydrolysis Lignin**
MP	Melting Point
BP	Boiling Point
AL	Alkaline lignin
GC	Gas Chromatography
MS	Mass Spectrometry
PLO	Pyrolytic Lignin Oil
HDO	Hydrodeoxygenation oil
LRCR	Lignin-Rich Corncob Residue
MW	Molecular Weight
LHV	Lower Heating Value
RON	Research Octane Number
CN	Cetane Number
P_{vap}	Vapor pressure
T_{melt}	Melting Temperature
T_{boil}	Boiling Temperature
H_{vap}	Enthalpy of vaporization

Summary

Deliverable 6.1 is the first one in task 6.1, whose goal is to characterize the composition of the fuels derived from enzymatic hydrolysis lignin (EHL) and to define the associated molecular substitutes. The first step is to identify the most important chemical species that present in EHL-derived solvolysis oil though bibliographic study and by the experimental analysis using two-dimensional gas chromatography (GC-2D) of samples provided by the EHLCATHOL partners. The results of the characterization are of particular importance in the case of the biofuels in the EHLCATHOL project and will make it possible to define molecular substitutes, which represent the main families of chemical species (e.g. alcohols, ketones, esters, phenolic compounds and arenes) to study the combustion properties on solvolysis oil.

This report provides general information on the lignins including EHL-derived solvolysis oils. In a first part, a general introduction on biomass valorization is given. In a second part, a bibliographical review of the experimental studies on the valorization of lignin and EHL is presented. In the third part, a bibliographical study on EHL-derived fuels combustion properties (BP, MP, RON and CN…) is displayed. In a fourth part, a review on kinetic works related to the gas-phase reactions of the main oxygenated aromatics expected in the biofuel composition is presented.

1. Introduction

Population growth and industrial development are leading to a rapid increase in the consumption of traditional fossil fuels, which poses major energy problems. The processing technology of lignocellulosic materials is not yet fully established. Although much progress has been made, second generation biorefineries will have to face great challenges over the next decade to become a mature and competitive technology.

Biomass is mainly composed of three polymers: cellulose, hemicellulose and lignin (1). Figure 1 presents the structure of cellulose and hemicellulose (which are polysaccharides) as well as the aromatic monomers present in lignin.

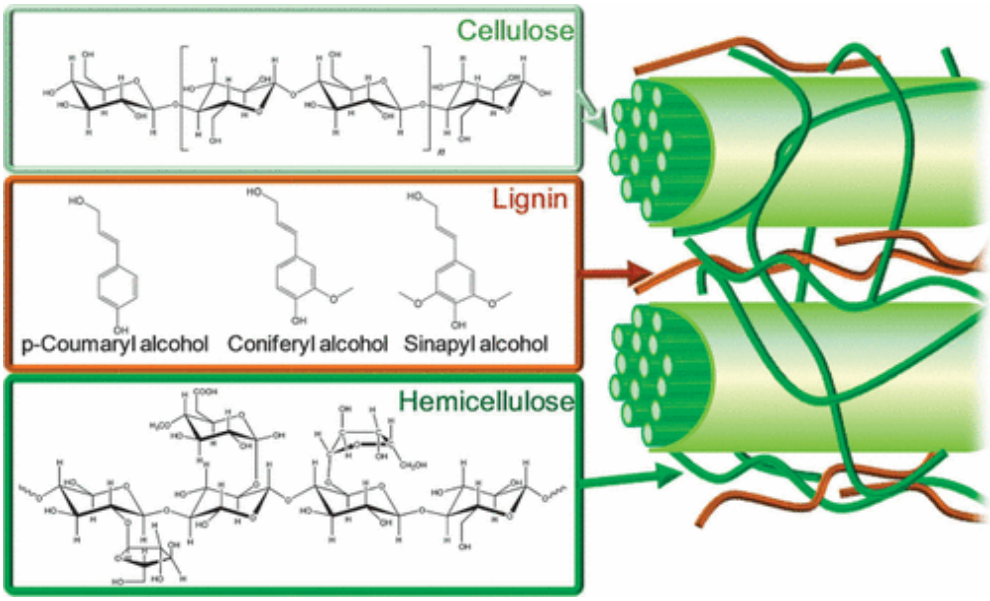

Figure 1: Components of lignocellulosic biomass (2).

1.1. Cellulose

Cellulose is composed of a linear polymer of glucose. It is the most abundant polysaccharide available on earth with a global stock of 100 billion tons. It is used in the paper/biorefinery industry and in the pharmaceutical field for additive synthesis.

1.2. Hemicellulose

Hemicellulose is composed of different monosaccharides such as hexoses and pentoses. The composition in hemicellulose is very variable depending on the sources of biomass. Figure 2 displays the main monosaccharides, which enters in the composition of hemicellulose (3).

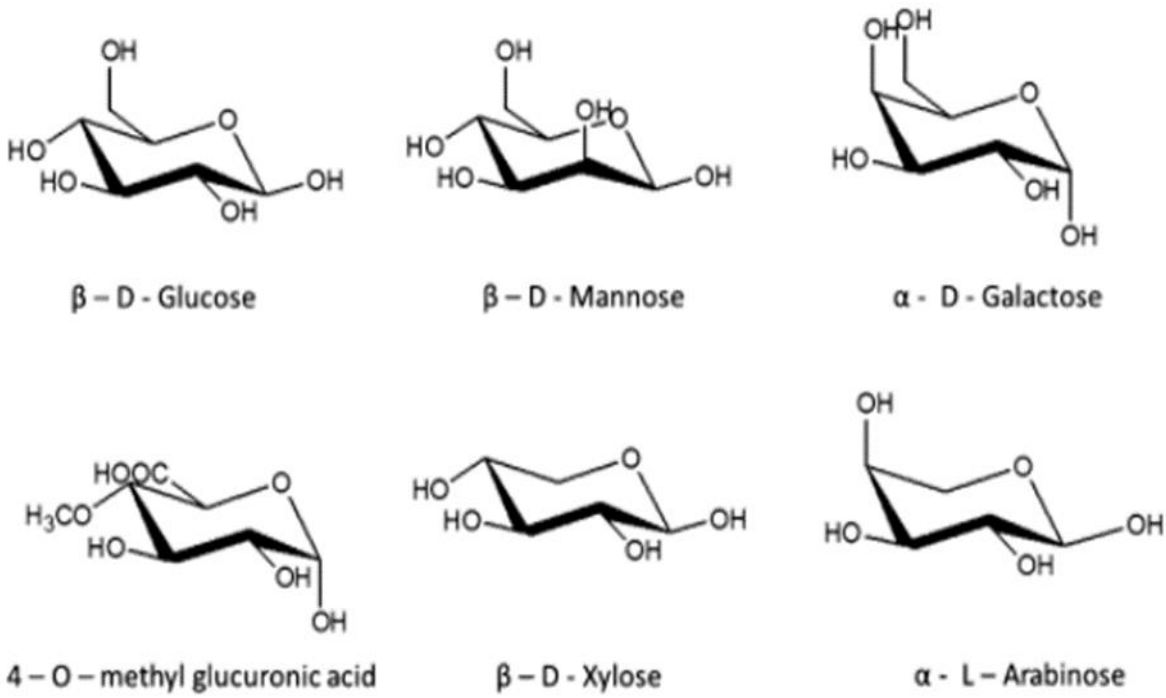

Figure 2: Representative monosaccharide molecules in hemicelluloses (3).

1.3. Lignin

Lignin is mainly found in the cell wall of woody plants and accounts for about 15–30% of the total lignocellulosic biomass. It is linked to hemicellulose, which confers mechanical strength to the cell wall and by extension the plant as a whole. It is the most abundant aromatic polymer in nature and is used for production of aromatic chemicals (4,5)

As shown in Figure 3 and 4 lignin is a complex and amorphous compound made up of phenolic units, such as hydroxyphenyl (H unit), guaiacyl (G unit) and syringyl (unit S), linked in various ways (6). The composition of lignin differs according to the type of wood. For conifers, lignin consists almost exclusively of guaiacyl (G) units, whereas for hardwoods, lignin is formed by a large number of syringyl units (S) (7).

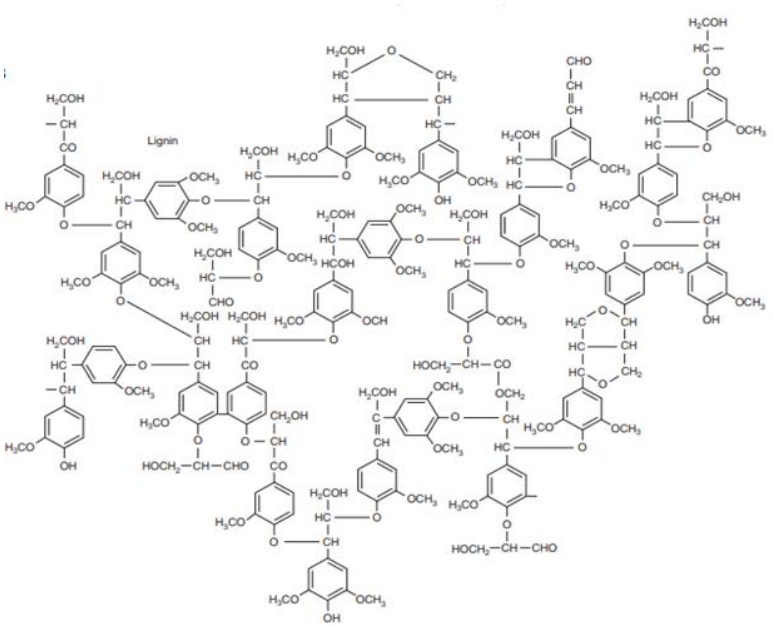

Figure 3: Example of the chemical structure of lignin (8).

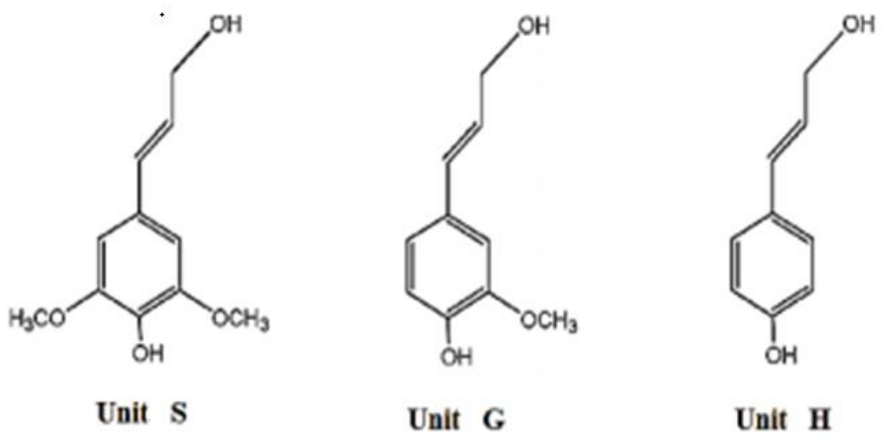

Figure 4 : Lignin structural units (9).

Indeed, the valuation of inedible lignocellulosic biomass has been the subject of great interest because of its potential to replace fossil resources for production of high added-value products. This biomass is also a source of lignocellulosic bioethanol because it contains glucose units that, once extracted, can be transformed into ethanol by fermentation.

The procedure of bioethanol production is mainly divided into four processes (see Figure 5):

1) Pretreatment, where the cellulose and hemicellulose of the biomass are made accessible
2) Enzymatic hydrolysis, where the biomass is converted into sugars
3) Fermentation, where the alcohol is produced from C_5 and C_6 monomers and, finally distillation to produce a purified liquid fuel.

The enzymatic hydrolysis or saccharification is one of the most critical factors in lignocellulosic biofuel production and represents one of the main technology development areas. However, enzymatic hydrolysis represents the second main operational cost, after the biomass production; in the second generation process (2G: the production of liquid biofuels from feedstocks not used for human consumption) it is ~25–30% of the operational costs, whereas in first generation process (1G) it is below 3%.

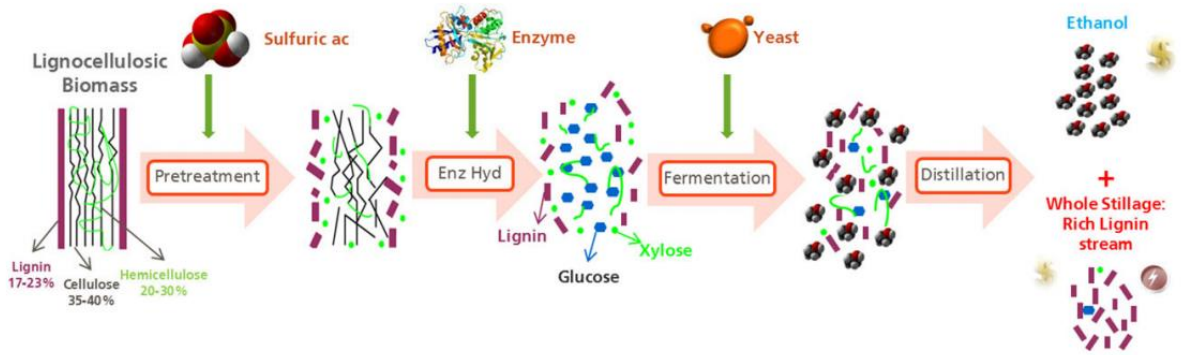

Figure 5: Lignocellulosic process converting the biomass into biofuels and coproducts. Process step for conversion of agricultural residues into ethanol. Source: (10).

1.4. Enzymatic hydrolysis lignin

Enzymatic hydrolysis lignin (EHL) is a by-product of the bioethanol production process (as described previously), which includes different steps (Figure 6). EHL has various active groups such as benzene rings, phenol hydroxyl and ether bonds (11).

EHL is insoluble in water at neutral pH, reducing its application in industry (12). In order to increase its possible use, studies have been carried out to improve its characteristics, and in particular its solubility in water (13).

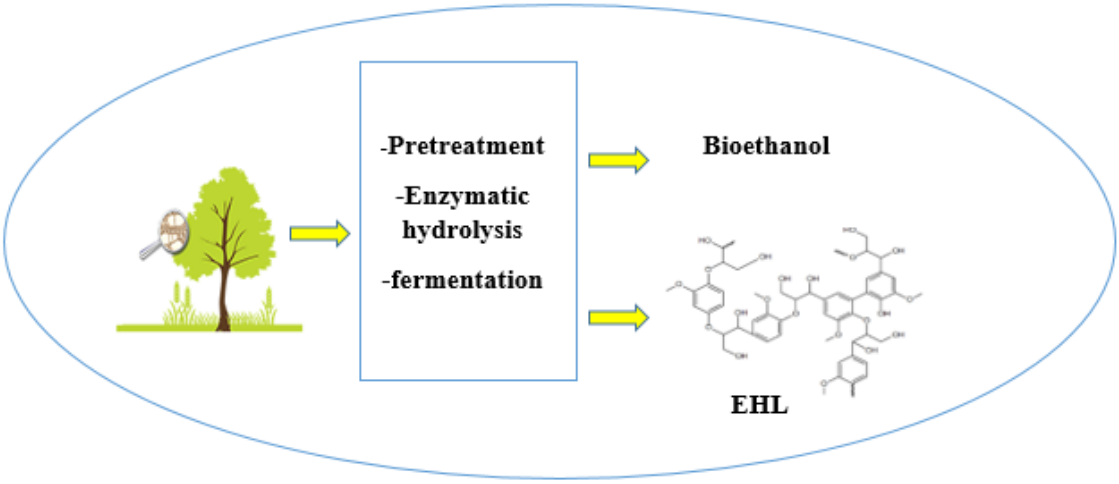

Figure 6: Schematic representation of the process of obtaining EHL

EHL is the byproduct of the 2G bioethanol process, either as the lignin fractionated during enzymatic hydrolysis or as the fermentation residue. The extraction of lignin is done without using harsh chemicals, thus makes it possible to better preserve the chemical structure of EHL than in alkaline lignin, Kraft lignin, lingosulfonate or organosolv lignin, which are obtained by pulping processes. Table 1 summarizes the different types of lignin samples and how they are obtained. Table 2 shows the property differences between EHL and the alkaline lignin (AL) derived from alkaline pulp manufacturing processes. Moreover, EHL allow much greater flexibility in optimizing its characteristics desirable for specific applications than traditional pulping processed lignin. Although Kraft pulp-derived lignin are now much closer to the market, the potential volume of biorefinery lignins like EHL is one to two orders of magnitude higher in the near future, if sugar/bioethanol biorefinery concepts are fully realized (13).

Table 1: Types of common lignin obtained from different process of biomass

Type of Lignin	Definition
Kraft lignin	Obtained from kraft pulp, which accounts for about 85% of the total lignin production in the world
Organosolv lignin	Extracted by Organosolv process, which uses numerous organic or aqueous solvent mixtures, such as methanol, ethanol, acetone, ethylene glycol
Soda lignin	Extracted from Bambusa Bambos using a Soda pulping process
Alkaline lignin	Derived from alkaline pulp manufacturing processes
Enzymatic hydrolysis lignin (EHL)	Lignin fractionated during enzymatic hydrolysis or as the fermentation residue of the 2G bioethanol process

Table 1: Property differences between EHL and AL

Property	EHL	AL
Molecular weight	Lower than AL (14)	Hundreds to millions (15)
Actives groups	Phenol hydroxyl, ether and ester bond, etc (11)	Phenolic hydroxyl, alcohol hydroxyl, carboxyl, ether bond, etc (16)
Purity	Relatively high (17)	Low (17)
Non-saturation	Relatively high (18)	Low (18)

To conclude, EHL is a specific type of lignin with particular properties, which relatively differs from other types of lignin. Its chemical structure is relatively preserved due to the mild reaction conditions used in the bio process and this has a great impact on the composition of the bio-oil, which is produced from EHL. Note that the lignin type is not the only factor affecting the composition of the bio-oil: the way the lignin is processed (catalyst, solvent and reaction conditions/atmosphere) has also a huge impact of the final composition of the bio-oil. These points are addressed in the next section of the deliverable.

2. Bibliographic review of experimental studies on the valorization of lignin and EHL to the production of bio-oils.

Lignin has received a lot of attention in recent years as a sustainable precursor because it is a large renewable source of aromatics, naphthenes and phenolic compounds. Compounds from the use of lignin and EHL can also reduce our dependence on fossil fuel feedstocks in the chemical industry.

The following section presents, literature studies on lignin upgrading and EHL to produce high performance fuel blends.

2.1. Lignin valorization to biofuels

The ability of lignin to break down into low molecular weight monomeric compounds has been studied extensively. The study of the different ways of exploiting lignin such as alkaline oxidation hydrolysis, alkaline fusion, alkaline demethylation, depolymerization, hydrogenolysis and pyrolysis, allows a better understanding of its use in the production of bio-oils.

De Wild et *al.* (19) reported a two-step process for the production of cycloalkanes and alkanes involving pyrolytic depolymerization of two types of lignin (GRANIT and Alcell lignin) followed by hydrotreatment on a Ru/C catalyst. Product analysis was performed by 2D-GC, GC-MS, and elemental analysis to obtain information on the effect of the hydrotreatment reaction on the molecular composition of the materials. The continuous pyrolysis of the two lignins resulted in a Pyrolytic Lignin Oil (PLO) and Hydrodeoxygenation oil (HDO). The compounds present in these bio-oils are summarized in Figure 7 that collected from ref. (19).

Class	Detected compounds	PLO	HDO oil	Structure
Phenolics	Phenol	0.49	0.00	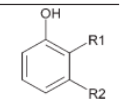
	3-methylphenol	0.69	0.00	
	2-methylphenol	2.03	0.00	
	3-ethylphenol	2.93	0.00	
	3-propylphenol	0.82	0.00	
Guaiacols	Guaiacol	1.66	0.00	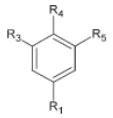
	2-Methoxy-5-methylphenol	2.62	0.00	
Syringols	2,6-dimethoxyphenol	3.28	0.00	
Methoxybenzenes	1,2,4-Trimethoxybenzene	4.43	0.00	
	Benzene, 1,2,3-trimethoxy-5-methyl-	1.25	0.00	
Catechols	Catechol	0.46	0.00	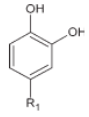
	3-Methoxycatechol	2.24	0.00	
Alkanes	Hexadecane	0.04	1.93	$R_1—(CH_2)_{14}—R_2$
	Pentadecane	0.03	0.50	
	Methylcyclohexane	0.00	0.26	
Cyclohexanols	Cyclohexanol	0.00	2.79	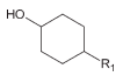
	Methylcyclohexanol	0.00	4.08	
	Ethylcyclohexanol	0.00	1.74	

Figure 7: Compounds, structures and percentage by weight detected in PLO and HDO oil (19).

Barta et *al*. (19) investigated the catalytic disassembly of an organosolv lignin using a Cu-doped porous metal oxide catalyst in supercritical methanol. The products obtained by this process are a complex mixture

composed mainly of monomeric substituted cyclohexyl derivatives with a significantly reduced oxygen content and a negligible aromatic compound one. These products can be further processed to produce liquid hydrocarbon fuels and additives.

Subsequently, the Weckhuysen group (21) and Jongerius et *al.* (22) reported on a two-step approach for the conversion of lignin into monomeric aromatic compounds. They demonstrated that the use of ethanol / water mixtures to dissolve the lignin significantly improved its solubility. They also observed that some of the monomers were ethoxylated and pointed out that this would reduce their tendency to repolymerize of formed monomers.

Following this work, Huang et *al.* (23) studied the use of ethanol to depolymerize alkaline lignin produced by an alkaline pulp process. They obtained a yield of 23% by weight of aromatics at 300 ° C under an N_2 atmosphere. Most of the aromatic products obtained are deoxygenated with various degrees of cyclic alkylation with methyl and / or ethyl groups. They also confirmed that a wide range of linear products (mainly alcohols and higher alkyl esters) can be formed in the presence of ethanol as a solvent, doing the same reaction without catalyst under similar conditions. The results of studying the effect of catalyst, solvent and reaction time are shown in Figure 8. $CuMgAlO_x$ catalyst exhibits excellent deoxygenation and low cycle hydrogenation activity.

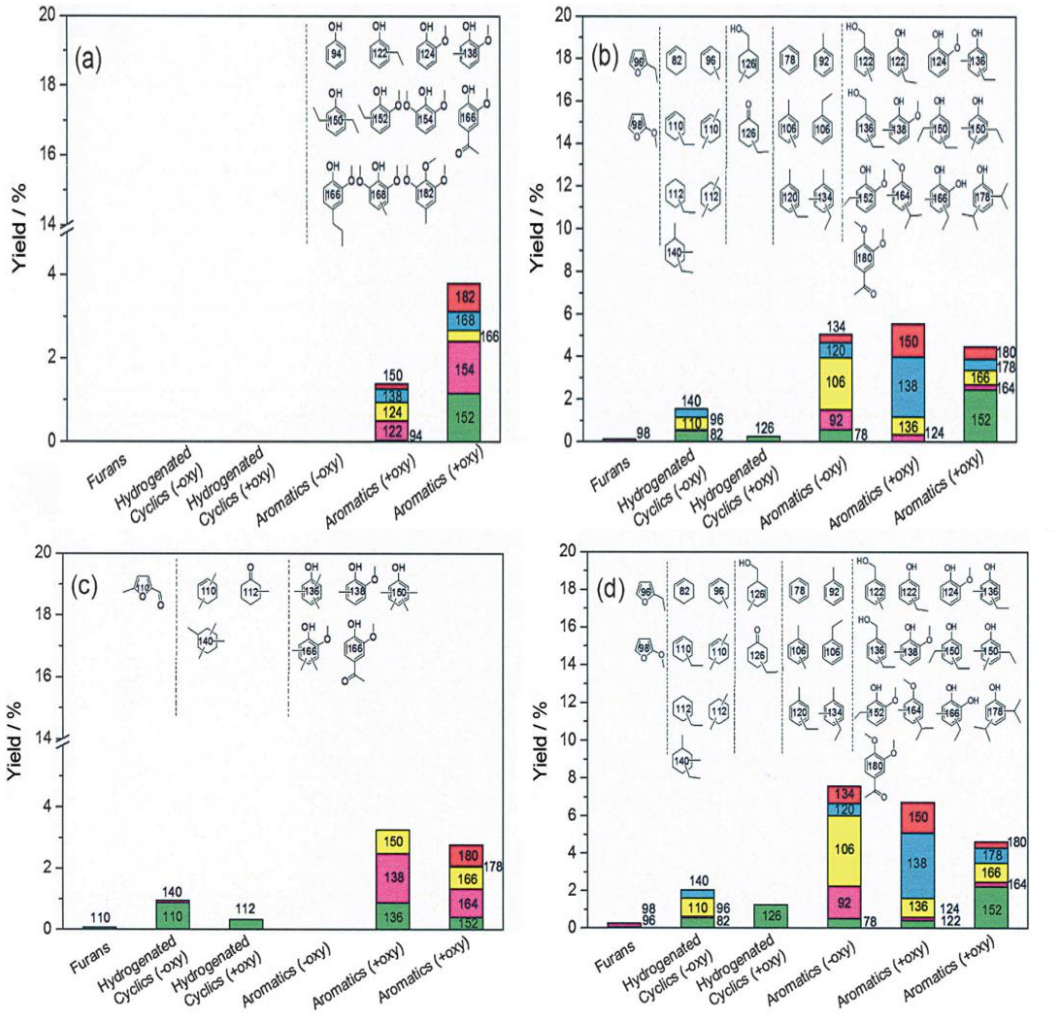

Figure 8: Distribution of the products for different reactions: (a) blank reaction at 300°C for 4 hours in ethanol, (b) CuMgAlOx at 300°C for 4 hours in ethanol, (c) CuMgAlOx at 300°C for 4 hours in methanol, (d) CuMgAlOx at 300°C for 8 hours in ethanol (24).

Li and coworkers (Ma et *al*. (22); Ma et *al*. (23); Chen et *al*. (26); Yan et *al*. (27), reported the depolymerization of Kraft lignin in ethanol with a number of Mo-based catalysts e.g., MoS_2, Mo_2C, $NiMo/Al_2O_3$, MoC_{1-x}/Cu-$MgAlO_Z$ and Mo_2N/Al_2O_3. Besides that, they confirmed that MoO_3 catalyst is highly selective for the cleavage of C-O bonds and possesses excellent regeneration property via calcination for removing deposited carbon on catalyst support compared to other Mo-based catalysts. The depolymerization of lignin, aims to give chemicals of high value of low molecular weight with a maximum overall yield of the most abundant liquid products. They confirmed that ethanol is an effective solvent for the reaction, which degrades the Kraft lignin into a mixture of small molecules and molecular fragments of intermediate size with molecular weights of around 700–1400. The reaction without hydrogen in the initial gas phase preceded much more efficiently than that with hydrogen, proving that it has a negative effect on the formation of low molecular weight products.

Figure 9 displayed the nature of species obtained from the ethanolysis of Kraft lignin in supercritical ethanol over different molybdenum oxide samples (26).

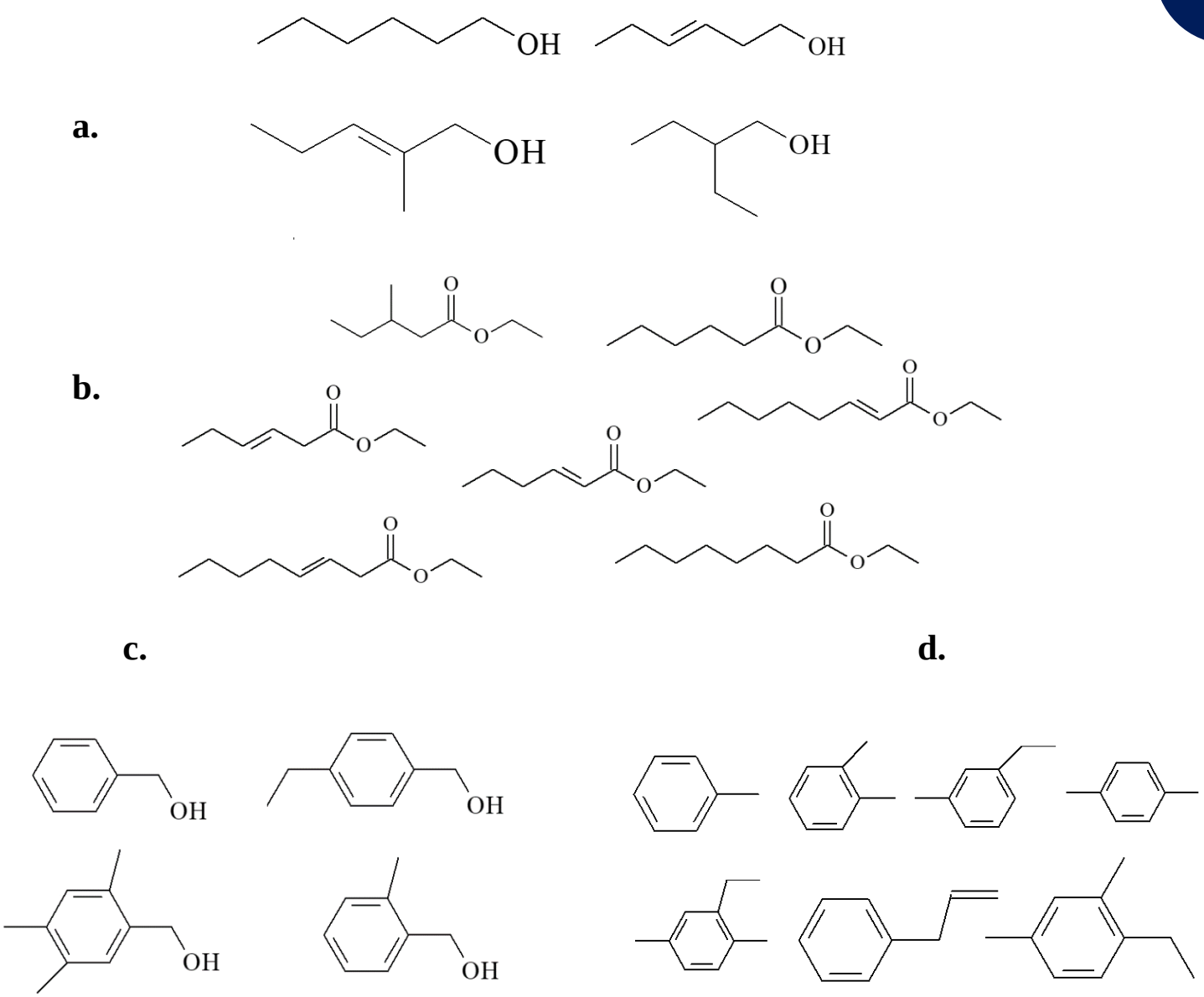

Figure 9: Summary of quantified products obtained from the ethanolysis of Kraft lignin in supercritical ethanol over different molybdenum oxide samples: a. C6 alcohols; b. C8 and C10 Esters; c. Benzyl alcohols and d. Arenes (26).

Huang et *al*. (27) investigated the role of Cu−Mg−Al mixed oxides in depolymerization of soda lignin in supercritical ethanol (Figure 10). This lignin is depolymerized and the products obtained are then converted by reactions of alkylation, hydrodeoxygenation and hydrogenation. To summarize, the proposed reaction network and the required active sites for lignin depolymerization in supercritical ethanol are shown schematically in Figure 10. The hydrogen produced by dehydrogenation reactions is involved in hydrogenolysis reactions of the chemical bonds in lignin and also to deoxygenate the monomeric and oligomeric products.

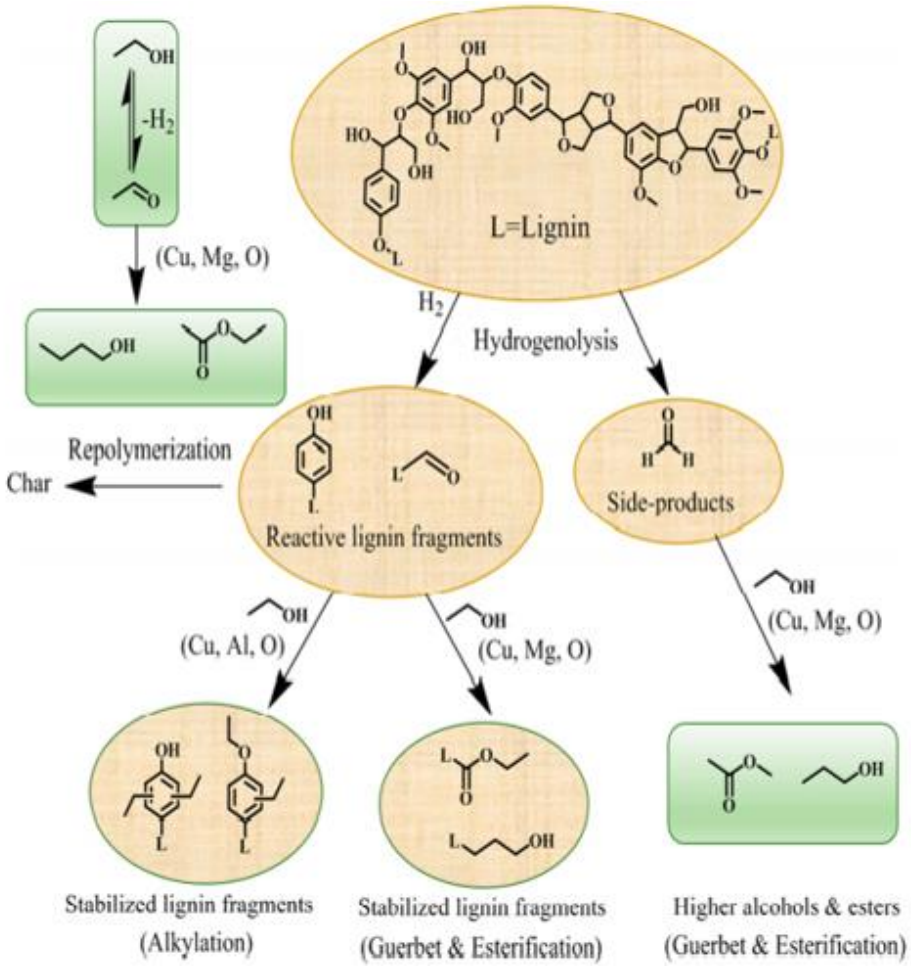

Figure 10: Proposed Reaction Network of Catalytic Depolymerization of Lignin in Ethanol over the CuMgAl(y) Catalysts (26).

Chesi et *al*. (28) used Raney-Ni for the depolymerization of poplar lignin in isopropanol/H_2O under an Ar atmosphere and obtained 12.9 wt % phenolic products and detected 0.8 wt % benzene ring saturated products.

Van den Bosch et *al*. (30) also investigated the activity of 21 wt % Ni/Al_2O_3 for the depolymerization of birch wood lignin in methanol and found that the mass transport limitation of the support reduced the monomer yield. Figure 11 shows the proposed mechanism of cleavage of the solvolytic β-O-4 bond in methanol via an α-methoxylated β-O-4 intermediate. The formation of units of coniferyl / sinapyl alcohol in the absence of Ni-Al_2O_3 implies the presence of a non-catalytic reduction step, suggesting that methanol acts as a hydrogen donor. Finally, the catalytic hydrogenation of unsaturated intermediates is crucial to avoid repolymerization into a condensed lignin product.

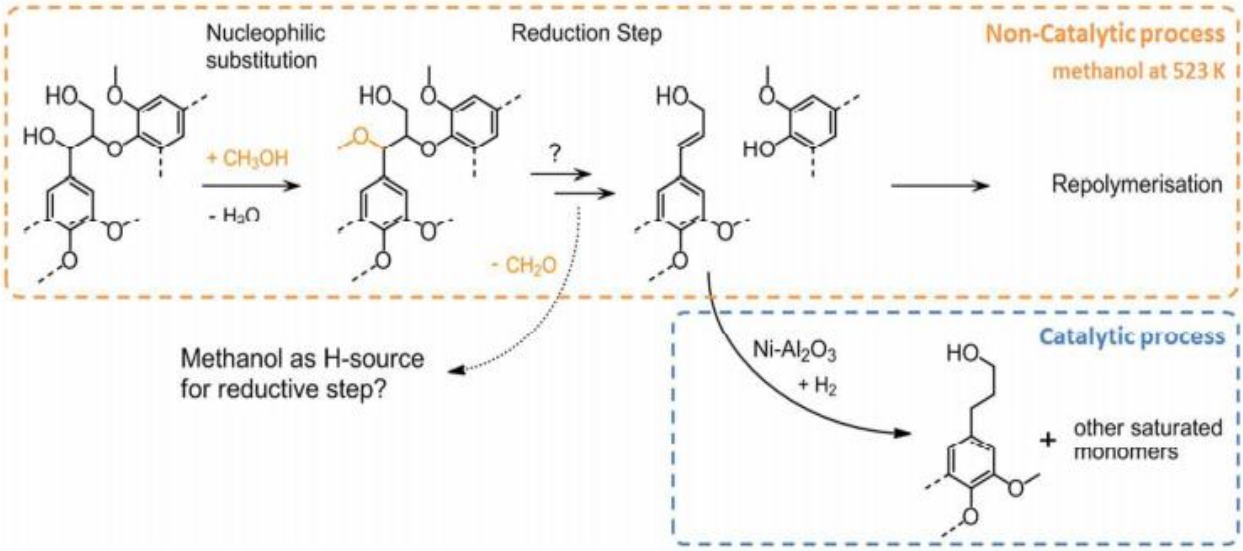

Figure 11: The mechanism of solvolytic β-O-4 bond cleavage in methanol through an α-methoxylated β-O-4 intermediate (30).

Korányi et *al*. (31) reported for the first time a substantial synergy between CuMgAl-oxide catalyst and nickel (phosphide) catalysts in the depolymerization of lignin in supercritical ethanol under optimized conditions. They obtained the best overall performance by combining CuMgAlOx with Ni_2P/SiO_2, resulting in a yield of 53% by weight of lignin monomers. The most important aspect is that the Ni-based phases are involved in the hydrogenation of reactive intermediates released from lignin by the action of the $CuMgAlO_x$ catalyst. Such reactive intermediates contain aldehyde and olefinic groups, which are in involved in condensation reactions that decrease the lignin monomer yield.

More recently, Tymchyshyn et *al*. (32) have prepared various catalysts supported on carbon and used them in the hydrotreatment of guaiacol as a model compound for lignin. The results indicated an improvement in the depolymerization of lignin, and the optimization study reveal that the initial temperature and pressure of hydrogen have a greater effect on the conversion of guaiacol than the reaction time.

In order to selectively convert lignin to alkanes, Qin et *al*. (33) thought of using a highly efficient catalytic process by introducing Pt and Ni based catalysts. However, the hydrodeoxygenation (HDO) oil of lignin to arenes or alkanes involves the depolymerization and hydrogenation of the aromatic polymer as well as the subsequent deoxygenation of the phenolic groups. For this, they developed a very efficient catalytic process for the conversion of an unprecedented high concentration of lignin to stable cyclic alkanes by introducing Pt/HAP into Ni/ASA catalyst in a dodecane media (Figure 12). It was found that Ni /ASA catalyst, reached a yield of ca. 40.4% by weight of C_3-C_{15} liquid alkane for a conversion of 25 g /L lignin in a one-pot process.

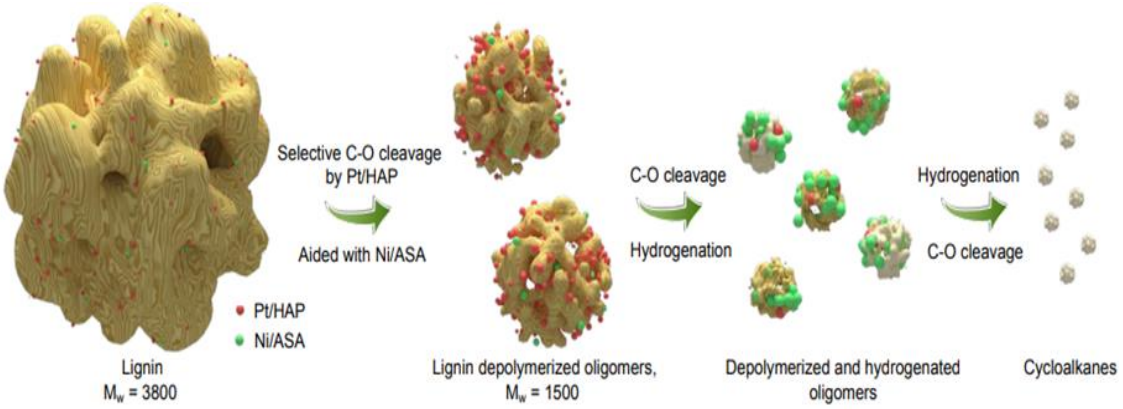

Figure 12: The strategy used for the conversion of high concentrated lignin to cyclic alkanes (33).

To summarize, lignin break-down into low molecular weight monomeric compounds has been intensively studied. The composition of bio-oils formed from lignin is highly dependent on the feedstock but also process conditions, in particular the catalyst type and the solvent. Several studies pointed out that the monomers could repolymerize and that upgrading (e.g., catalytic hydrogenation) could solve this problem. The major products obtained in the above-mentioned studies are presented in Table 3.

Table 2: The main products obtained in the reported lignin studies

Family	Compounds
Benzyl alcohols	Phenol , Guaiacol , Syringyl, Catechol , Cresol , Toluene
Alcohols	Methanol, Ethanol, Butanol, Benzyl alcohol
Esters	Methyl methacrylate , Dibutyl phthalate, Methylpyruvate
Arenes	Benzene and Alkyl-benzenes

2.2. Enzymatic hydrolysis lignin valorization to biofuels

In recent years, the growth of the bioethanol industry has made it possible to produce large quantities of EHL. But a large amount of this EHL is incinerated for on-site energy production.

The following section presents literature studies on the conversion of EHL to produce high performance fuel blends, i.e., high heating value jet-fuel, high octane number gasoline and high cetane number diesel fuels. The reaction time, the solvent, the temperature, and the initial hydrogen pressure are the parameters studied as they have significant effects on the products resulting from the valorization of EHL.

Wang et *al*. (34) studied the depolymerization of EHL in methanol at 240°C for 4 h with 3 MPa H_2 and they obtained an aromatic monomer yield of 12.1% by weight. They used for earth-abundant Ni catalyst supported on activated carbon (Ni/AC). The used catalyst is easily collected from the reaction solution by an external magnet and reused up to six times without loss of catalytic reactivity, which offers an alternative to develop very efficient heterogeneous product catalysts.

Bai et *al*. (35) investigated the depolymerization of lignin-rich corncob residue (LRCR, a kind of EHL) in supercritical ethanol on a NiMo alloy catalyst on a support of alumina (NiMo/Al). They examined the effect of reaction conditions on the depolymerization of LRCP, such as reaction temperature, initial hydrogen pressure, and solvent. They found that the highest overall aromatic yield, 255.4 mg/g of LRCR, is achieved at 320 °C for 7.5 h under 27.6 bar of hydrogen pressure in supercritical ethanol, and the LRCR was completely converted to aromatics efficiently without the formation of tar or char in the reactor and on the catalyst surface. Catalytic depolymerization of LRCR likely occurred as shown in Figure 13. A total of 17 aromatic compounds were identified and specified as the main products. The structures of these identified molecules are shown in Figure 14.

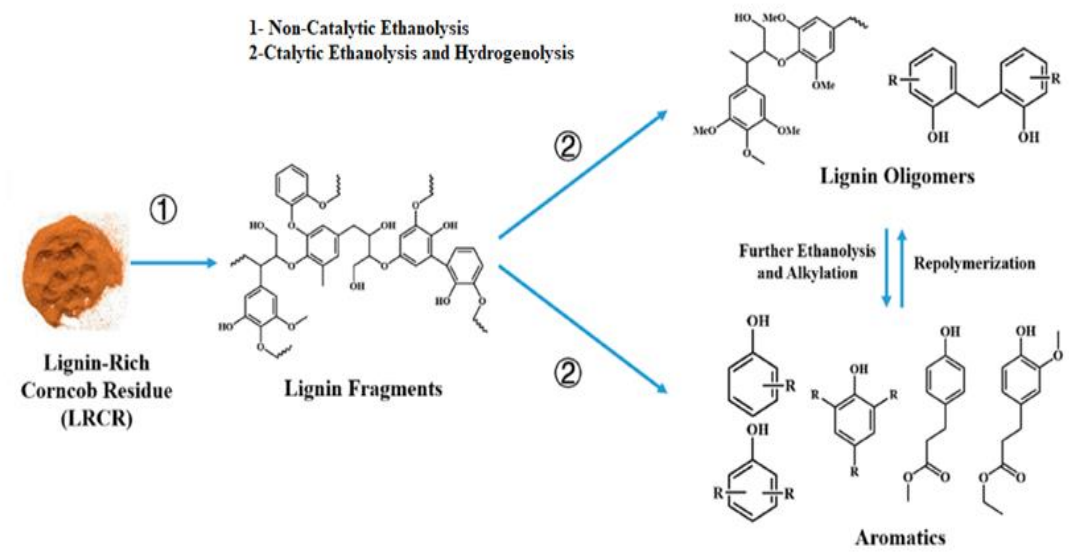

Figure 13: Possible Reaction Pathway for LRCR Depolymerization (35).

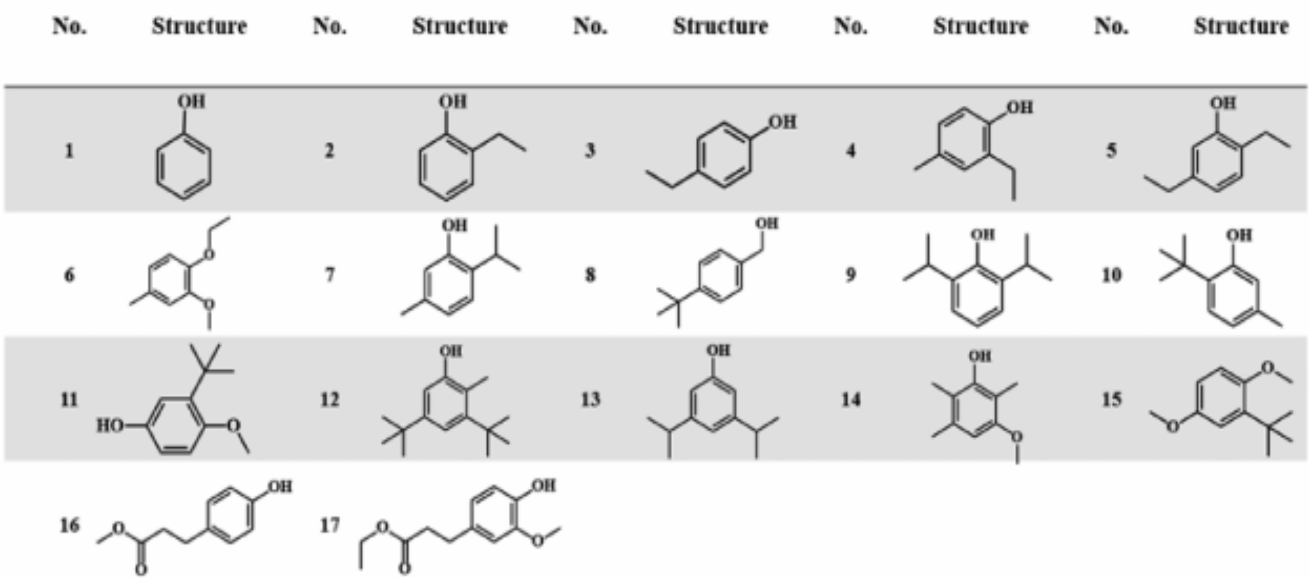

Figure 14: Identified molecular structures in liquid products from depolymerization of LRCR in supercritical ethanol (35).

After that, Mai et *al*., (36) studied the conversion of EHL in supercritical ethanol over a $WO_3/\gamma\text{-}Al_2O_3$ Catalyst, at 320 °C for 8 h. As shown in Figure 15, besides depolymerized EHL products, two aliphatic compounds such as aromatic ethers/esters and alkyphenols, propionic ether and 3-butenylethyl ether were formed, which were confirmed to be formed from ethanol by a blank reaction (without EHL)). They also studied the depolymerization of EHL in supercritical methanol and isopropanol, the results of which showed that ethanol was the most efficient solvent.

No.	Structure	Yield	No.	Structure	Yield	No.	Structure	Yield	No.	Structure	Yield
1		39.4	7	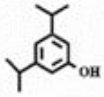	3.1	13	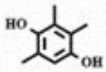	5.3	19		5.4
2	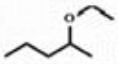	8.2	8		6.5	14		89.3	20	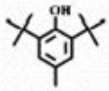	12.7
3		-	9	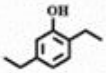	13.0	15	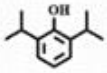	11.6	21	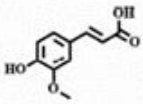	5.7
4		4.9	10	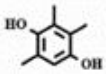	7.7	16	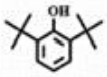	10.3	22	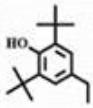	13.0
5		13.8	11	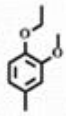	13.7	17	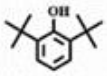	4.6	23		26.3
6	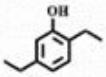	6.6	12	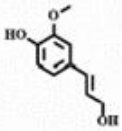	9.3	18	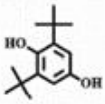	15.3	24	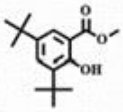	37.6

Figure 15: Structures of identified molecules obtained from depolymerization of EHL over a $WO_3/\gamma\text{-}Al_2O_3$ at 320°C (36)

More recently, Sang et *al*. (37) provided an effective new strategy for a better valorization of EHL, adjusting Ni microstructure to increase the number of active sites to improve its reactivity. Indeed, they prepared a number of unsupported nickel-based catalysts for the depolymerization of EHL in a batch reactor at 280°C for 6 h. They found that Ni (220H), which was prepared from the decomposition of nickel formate at 220°C in hydrogen, allowed the liquefaction of EHL and the highest monomer yield of 28.5%. This study showed that the different activities of the fabricated nickel-based catalysts on EHL can be caused by the different particle size of Ni, and the smaller the Ni particles, the higher the activity of the catalyst. Aromatic esters and para-propanol substituted phenols were the main detected products, as shown in Figure 16.

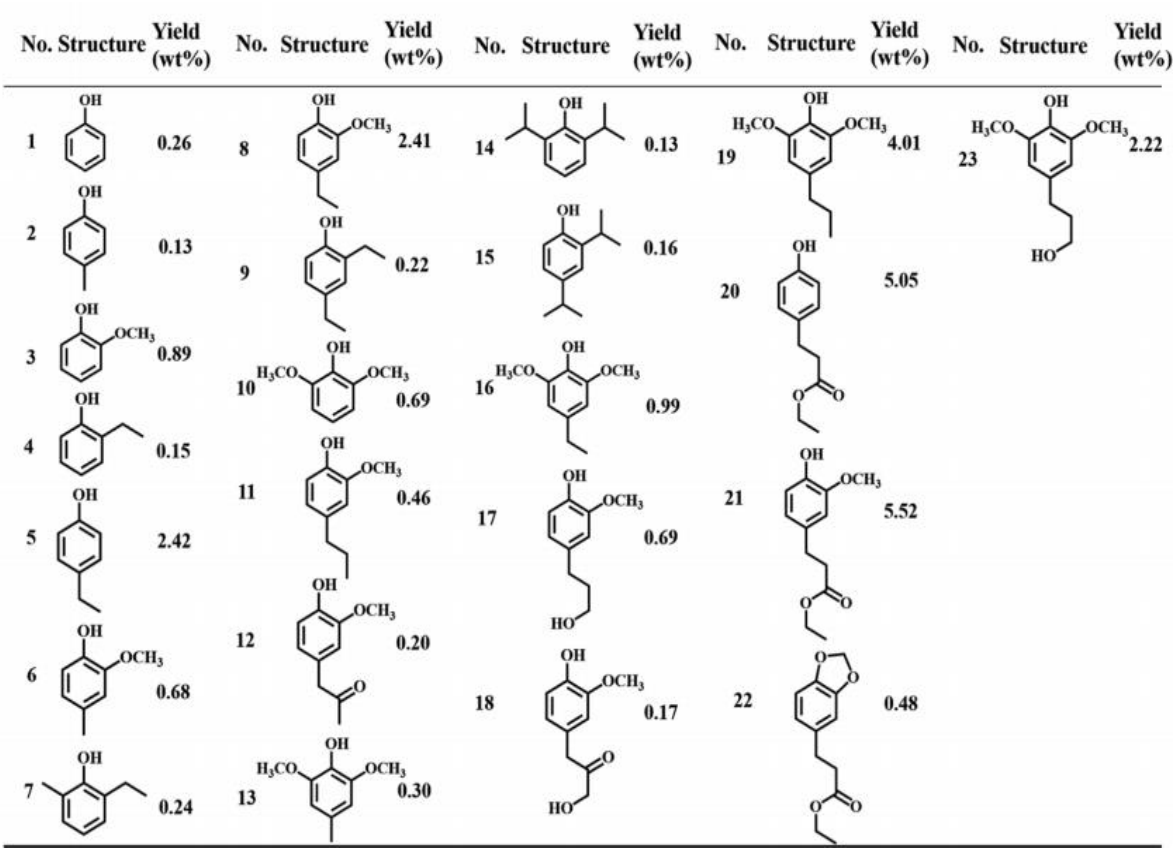

Figure 16: Structures of identified molecules obtained from depolymerization of EHL over an unsupported Nickel catalyst at 280°C (36).

Later, Tymchyshyn et *al*. (38) investigated the reductive depolymerization of EHL in supercritical acetone and in the presence of a catalyst under a hydrogen atmosphere to obtain low molecular weight compounds. They chose acetone as the solvent because the aromatic components of EHL and the aliphatic compounds produced are expected to be soluble in acetone. The MoRu/AC catalyst produced a bio-oil at 320°C with a substantially increased H/C ratio and <2 wt % solid residue, suggesting an excellent hydrogenation/hydrodeoxygenation activity of the MoRu/AC. The results show that the phenolic compounds are the main component in bio-oils produced.

In the work planned by Aalto University and TU/e in the EHLCATOL project in order to convert completely the enzymatic hydrolysis lignin (EHL) via catalytic solvolysis for making high-valued fuel commodities like gasoline, jet fuel and diesel range molecules, fuel compatible solvents such as lower chain alcohols (from C_1 to C_4) and/or C_6-C_8 alkanes will be used. Moreover, highly efficient supported catalysts with low-cost non-noble metals like Ni, Mo, Fe and/or their alloys, will be utilized to enhance the molecules in gasoline, jet fuel and diesel ranges. The experiments will be performed in a ~50-100 mL batch reactor equipped with a magnetic stirrer, sampling lines, pressure gauge and heating mantle. The EHL experiments typically performed in presence of suitable solvents at the temperature range of 250-350°C with/without H_2, N_2 or Ar (with initial pressure of 2-0-4.0 MPa) for 3-6 h. Here is a list of solvents, which might be envisaged:

- Water
- Methanol
- Ethanol
- 1-Propanol

- iso-Propanol
- 1-Butanol
- 2-Butanol
- iso-Butanol
- tert-Butanol
- Ethylene glycol
- Glycerol
- Acetone
- Methyl ethyl ketone
- Ethyl acetate
- 1,4-dioxane
- Tetrahydrofuran
- Diethyl ether
- Cyclohexane
- n-Hexane
- n-Dodecane

To summarize, the valorization of EHL through the formation of bio-oils has a great potential and benefits from the past researches on other types of lignins. The composition of EHL derived bio-oils is highly dependent on the process conditions like the catalyst, the solvent the temperature and reaction atmosphere. _For instance, working under hydrogen atmosphere enables to increase the H/C ratio through hydrogenation and hydrodeoxygenation processes.

As far as the composition of the obtained biofuels is concerned, the **oxygenated aromatics** are always the most important fraction, but **arenes** should also be considered, as well as **the** remaining presence of the **used solvents** and **the compounds, which might be derived from those solvents** through the catalytic process (e.g., esters).

3. Bibliographical study on EHL-derived fuels and their combustion properties

This part covered the global properties of biofuel's potential components: mainly oxygenated aromatics, arenes, which are previously described as lignin catalytic solvolysis products.

The Molecular Weight (MV) and density are widely used in physics and chemistry; however, Lower Heating Value (LHV), Research Octane Number (RON) and Cetane Number (CN) are widely used in combustion characteristics:

- LHV: Thermal energy released during combustion considering all products in their gas state,

- RON: index characterizing self-ignition capacity of gasoline. Values are defined in respect of reference species: *n*-heptane (RON=0) and *iso*-octane (RON=100),

- CN: index characterizing self-ignition capacity of diesel. Values are defined in respect of reference species: α-methylnaphthalene (RON=0) and *n*-cetane (RON=100).

These data of surrogates may be interpolated to predict fundamental biofuel properties. The data shown in Tables 4, 6, 8, 10 are global quantities deduced directly from the species known formulas (MW, density, LHV) or data taken from literature (RON, CN), which will be used as a data base to develop theoretical and numerical tools for properties prediction in WP6.2.

Phase change data (Tables 5, 7, 9, 11) are also needed to anticipate constraints during experiments, such vapor pressure (P_{vap}) or the phase change state parameters at ambient temperature and pressure, boiling temperature (T_{boil}), melting temperature (T_{melt}) and the enthalpy of vaporization (H_{vap}). Globally, these parameters will help us to choose the suitable experimental conditions and to adapt our facilities in WP6.3 and WP6.4.

Table 4: Global properties of oxygenated aromatics.

	MW g/mol		**Density (25°C)** kg/m³		**LHV** MJ/kg		**RON**		**CN**	
	Value	Ref	Value	Ref	Value	Ref	Value	Ref	Value	Ref
Guaiacol	124.1	(39,40)	1129	(41,42)	27.5	(41–44)			19	(41,42,45)
Anisole	108.1	(39,40)	980	(39,42,46)	33.7	(41–44,46–50)	114	(41,42,47,48,51)	6	(41,45,52)
Phenol	94.1	(39,40)	1065	(39,42)	31.3	(42)				
o-cresol	108.1	(39,40)	1028	(39)	32.7[1]	(40,53)			75	(54)
p-cresol	108.1	(39,40)	1140	(39,42)	29.6	(42)	153	(42)	75	(54)
m-cresol	108.1	(39,40)	1030	(39)	32.8[1]	(40,53)			75	(54)
Catechol	100.1	(39,40)	1344[2]	(55)	27.7[3]	calc.				
Benzyl alcohol	108.1	(38,39)	1041	(38)	34.55	(85)			29	(85)
2-phenyl ethanol	122.2	(39,41)	1017	(86)	35.0	(41,42,44,57,58)	116	(43,44,48,57)	8	(48,54)

[1] *LHV calculated from enthalpy of combustion*

[2] *density at 20°C*

[3] *LHV calculated from enthalpy of formation (enthalpy of formation calculated with Joback's method (52)*

Table 5: Phase change data of oxygenated aromatics.

	T_{boil} (1atm) K		**T_{melt} (1 atm)** K		**P_{vap} (25°C)** bar		**H_{vap} (25°C)** kJ/kg	
	Value	Ref	Value	Ref	Value	Ref	Value	Ref
Guaiacol	478	(41–44)	301	(40,42)	$1.29\ 10^{-4}$	(39)	494.4	(39)
Anisole	427	(39–42,44,48)	250	(40,42)	$4.28\ 10^{-3}$	(39)	425.9	(39,40,47–49)
Phenol	455	(39,40,42)	314	(40,42)	$6.38\ 10^{-4}$	(39)	583.7	(39)
o-cresol	464	(39,40)	304	(40)	$4.88\ 10^{-4}$	(39)	508.9	(39)
p-cresol	475	(39,40,42)	307	(40,42)	$1.89\ 10^{-4}$	(39)	548.8	(39)
m-cresol	475	(39,40)	284	(40)	$2.74\ 10^{-4}$	(39)	526.4	(39)
Catechol	519	(39,40)	377	(40)	$3.57\ 10^{-6}$	(39)	696.2	(39)
Benzyl alcohol	478	(38,39)	257	(39)	$4.82\ 10^{-5}$	(38)	610.6	(38)
2-phenyl ethanol	493	(39,57,58)	254	(39)	$1.16\ 10^{-6}$	(93)	562.9	(41,44,57)

Table 6: Global properties of arenes.

	MW g/mol		**Density (25°C)** kg/m³		**LHV** MJ/kg		**RON**		**CN**	
	Value	Ref	Value	Ref	Value	Ref	Value	Ref	Value	Ref
Toluene	92.1	(39,40,56,57)	862	(39,56)	40.9	(41,43,57–60)	116	(41,42,47,61–65)	6	(41,45,47,63,66)
p-xylene	106.2	(39,40,57)	849	(39,67)	41.5	(44,48,57–60)	121	(44,61,63,64)	6	(63,66)
m-xylene	106.2	(39,40)	855	(39,67)	41.4	(59,60)	122	(44,63,64)	7	(63,66)
o-xylene	106.2	(39,40)	870	(39,67)	41.4	(59,60)	113	(44,63,64)	8	(63,66)
Styrene	104.2	(39,40)	901	(39)	41.5	(60)				
Ethyl benzene	106.2	(39,40,57)	855	(39,67)	41.4	(57–60)	108	(41,57,58,61,63)	6	(63,66)
1,2,3-tri methyl benzene	120.2	(39,40)	891	(39,40)	41.2[1]	(40)	110	(47,63,64)	10	(63,66)
1,2,4-tri methyl benzene	120.2	(39,40)	857	(39,40)	41.0	(59)	148	(64)	9	(47,63,66)
1,3,5-tri methyl benzene	120.2	(39,40)	842	(39,40)	41.2[1]	(40)	138	(63,64)	8	(63,66)
1,2-ethyl toluene	120.2	(39,40)	877	(39,40)	41.3[1]	(40)	101	(45,63)		
1,3-ethyl toluene	120.2	(39,40)	860	(39,40)	41.3[1]	(40)	102	(63)		
1,4-ethyl toluene	120.2	(39,40)	857	(39,40)	41.3[1]	(40)	102	(63)		
1,2-diethyl benzene	134.2	(39,40)	876	(39,40)	41.6[1]	(40)				
1,3-diethyl benzene	134.2	(39,40)	860	(39,40)	41.6[1]	(40)	103	(63)	5	(66)
1,4-diethyl benzene	134.2	(39,40)	875	(39,40)	41.6[1]	(40)	103	(45,63)		
2-propenyl benzene	118.2	(40)	892	(40)	42.0[1]	(40)				
2-ethyl 1,4-dimethyl benzene	134.2	(39,40)	873	(39,40)	41.5[1]	(40)	104	(45,63)		
1-ethyl 2,4-dimethyl benzene	134.2	(39,40)	872	(39,40)	41.5[1]	(40)	101	(63)		

[1] *LHV calculated from enthalpy of combustion.*

Table 7: Phase change data of arenes.

	T_{boil} (1atm) K		T_{melt} (1 atm) K		P_{vap} (25°C) bar		H_{vap} (25°C) kJ/kg	
	Value	Ref	Value	Ref	Value	Ref	Value	Ref
Toluene	383	(39–41,44)	178	(40)	$3.73\ 10^{-2}$	(39,40)	408.0	(39,40,57,58)
p-xylene	411	(39,40,48)	286	(40)	$1.13\ 10^{-2}$	(39,40)	396.9	(39,40,48,57,58)
m-xylene	412	(39,40)	225	(40)	$1.07\ 10^{-2}$	(39,40)	398.1	(39)
o-xylene	417	(39,40)	248	(40)	$8.58\ 10^{-3}$	(39,40)	403.6	(39)
Styrene	419	(39,40)	240	(40)	$9.91\ 10^{-3}$	(39)	403.5	(39)
Ethyl benzene	409	(39,40)	179	(40)	$1.25\ 10^{-2}$	(39)	413.2	(40,57,58)
1,2,3-tri methyl benzene	449	(39,40)	248	(40)	$1.84\ 10^{-3}$	(39)	404.0	(39)
1,2,4-tri methyl benzene	442	(39,40)	228	(40)	$2.49\ 10^{-3}$	(39)	395.4	(39)
1,3,5-tri methyl benzene	438	(39,40)	226	(40)	$2.85\ 10^{-3}$	(39)	394.1	(39)
1,2-ethyl toluene	438	(39,40)	190	(40)	$2.38\ 10^{-3}$	(39)	366.3	(39)
1,3-ethyl toluene	435	(39,40)	176	(40)	$4.70\ 10^{-3}$	(39)	379.8	(39)
1,4-ethyl toluene	435	(39,40)	210	(40)	$4.45\ 10^{-3}$	(39)	368.3	(39)
1,2-diethyl benzene	456	(39,40)	242	(40)	$1.40\ 10^{-3}$	(39)	355.3	(39)
1,3-diethyl benzene	454	(39,40)	189	(40)	$1.51\ 10^{-3}$	(39)	355.2	(39)
1,4-diethyl benzene	457	(39,40)	230	(40)	$1.29\ 10^{-3}$	(39)	369.9	(39)
2-propenyl benzene	429	(40)	233	(40)	$4.76\ 10^{-3}$	(68)	391.3	(68)
2-ethyl 1,4-dimethyl benzene	460	(39,40)	219	(40)	$1.26\ 10^{-3}$	(39)	376.1	(39)
1-ethyl 2,4-dimethyl benzene	462	(39,40)	210	(40)	$1.19\ 10^{-3}$	(39)	378.7	(39)

Table 8: Global properties of proposed solvents.

	MW g/mol		Density (25°C) kg/m³		LHV MJ/kg		RON		CN	
	Value	Ref	Value	Ref	Value	Ref	Value	Ref	Value	Ref
Methanol	32.0	(39,40)	787	(39)	20.3	(47,59,60,69,70)	110	(44,45,47,71)	3	(66)
Ethanol	46.1	(39,40,49,50,57)	800	(39)	27.3	(41,47–50,57–60,69,70,72,73)	109	(41,44,45,47,49,49,57,58,63,71,72)	9	(50,66,70,74)
1-propanol	60.1	(39,40)	805	(39)	30.7	(47,73)	103	(45,47)	12	(66)
Iso-propanol	60.1	(39,40)	787	(39)	30.7	(47)	108	(45,47,75)	12	(76)
1-butanol	74.1	(39,40)	794	(39)	33.2	(47,70,77,78)	99	(45,47,71,75,77)	17	(45,47,66,70,76,77)
2-butanol	74.1	(39,40)	811	(39)	33.1	(47)	107	(45,47,71,75)	9	(45)
Iso-butanol	74.1	(39,40)	793	(39)	33.2	(47,77)	109	(45,47,75,77)	9	(45,47)
Tert-butanol	74.1	(39,40)	761	(39)	32.6	(77)	105	(45,77)		
Ethylene glycol	62.1	(39,40)	1110	(39)	19.2	(40)				
Acetone	58.1	(39,40)	785	(39)	28.9	(59,78,79)	108	(75)	53	(80)
Methyl ethyl ketone	72.1	(39,40)	795	(39)	31.4	(47,81)	109	(45,47,71,75)		
Ethyl acetate	88.1	(39,40)	895	(39)	23.8	(47,49)	118	(47,49,71)		
1,4-dioxane	88.1	(39,40)	1029	(39)	25.0[1]	(40)				
Tetrahydrofuran	72.1	(39,40)	880	(39)	34.7	(40)	73	(45)	24	(45,82)
Diethyl ether	74.1	(39,40)	716	(39)	33.9	(70,83,84)			141	(66,70,74,83)
Cyclohexane	84.2	(39,40)	767	(39)	44.5	(60)	83	(45,47,63)	16	(45,47,63,66)
n-hexane	86.2	(39,40)	656	(39)	45.4	(60,72)	29	(45,47,72,75)	48	(45,47,63,66,85)
n-dodecane	170.3	(39,40)	750	(39)	44.6	(72)			79	(45,47,63,66,85,86)

[1] *LHV calculated from enthalpy of combustion*

Table 9: Phase change data of proposed solvents.

	T_{boil} (1atm) K		T_{melt} (1 atm) K		P_{vap} (25°C) bar		H_{vap} (25°C) kJ/kg	
	Value	Ref	Value	Ref	Value	Ref	Value	Ref
Methanol	338	(39,40)	176	(40)	$1.69\ 10^{-1}$	(39,40)	1193.3	(39,40,47)
Ethanol	352	(39,40,48,50)	159	(40)	$7.69\ 10^{-2}$	(39,40)	921.6	(39,40,47–49,57,58)
1-propanol	370	(39,40)	147	(40)	$2.80\ 10^{-2}$	(39,40)	774.3	(39,40,47)
Iso-propanol	355	(39,40)	186	(40)	$5.80\ 10^{-2}$	(39)	735.2	(39,40,47)
1-butanol	391	(39,40)	188	(40)	$8.98\ 10^{-3}$	(39,40)	682.9	(39,40,47)
2-butanol	372	(39,40)	158	(87,88)	$2.33\ 10^{-2}$	(39)	641.0	(39,40,47)
Iso-butanol	381	(39,40)	167	(40)	$1.39\ 10^{-2}$	(39)	660.0	(39,40,47)
Tert-butanol	356	(39,40)	298	(40)	$5.60\ 10^{-2}$	(39)	588.6	(39)
Ethylene glycol	470	(39,40)	261	(40)	$2.87\ 10^{-6}$	(39)	1302.0	(39)
Acetone	329	(39,40)	179	(40)	$30.6\ 10^{-1}$	(39,40)	538.4	(39)
Methyl ethyl ketone	353	(39,40)	186	(40)	$1.23\ 10^{-1}$	(39)	480.3	(39,40,47)
Ethyl acetate	350	(39,40)	190	(40)	$1.26\ 10^{-1}$	(39,40)	929.8	(39,40,47,49)
1,4-dioxane	374	(39,40)	285	(40)	$4.91\ 10^{-2}$	(39,40, 89)	433.3	(39,89)
Tetrahydrofuran	339	(39,40)	164	(40)	$2.16\ 10^{-1}$	(39,40)	439.1	(39,40)
Diethyl ether	308	(1,2)	154	(40)	$6.90\ 10^{-1}$	(39,40)	362.8	(39,40)
Cyclohexane	354	(39,40)	280	(40)	$1.30\ 10^{-1}$	(39,40)	387.9	(39,40)
n-hexane	342	(39,40)	178	(40)	$2.00\ 10^{-1}$	(39,40)	363.4	(39,40)
n-dodecane	489	(39,40)	264	(40)	$1.70\ 10^{-4}$	(39)	337.4	(39)

Table 10: Global properties of possible compounds deriving from the solvents after the catalytic process.

	MW g/mol		Density (25°C) kg/m³		LHV MJ/kg		RON		CN	
	Value	Ref	Value	Ref	Value	Ref	Value	Ref	Value	Ref
Hexan-1-ol	102.2	(39,40)	816	(39)	39.0	(90)	69	(45)	23	(66)
2-ethyl butanol	102.2	(39,40)	829	(39)	36.0[3]	calc.				
3-hexen-1-ol	100.2	(40)	817	(87)	34.5[3]	calc.				
2-methyl-2-penten-1-ol	100.2	(40)			35.5[3]	calc.				
2-methylphenyl methanol	122.2	(40)	1028	(87)	34.1[3]	calc.				
4-ethyl phenyl methanol	136.2	(40)			35.1[3]	calc.				
2,4,5-trimethyl phenyl methanol	150.2	(40)			35.7[3]	calc.				
Ethyl heptanoate	158,2		870		32.9[3]	calc.				

[3] *LHV calculated from enthalpy of formation (enthalpy of formation calculated with Joback's method (52)*

Table 11: Phase change data of possible compounds deriving from the solvents after the catalytic process.

	T_{boil} (1atm) K		T_{melt} (1 atm) K		P_{vap} (25°C) bar		H_{vap} (25°C) kJ/kg	
	Value	Ref	Value	Ref	Value	Ref	Value	Ref
Hexan-1-ol	430	(39,40)	225	(40)	$1.24\ 10^{-3}$	(39)	552.1	(39,40)
2-ethyl butanol	421	(39,40)	258	(87)	$2.04\ 10^{-3}$	(39)	524.3	(39)
3-hexen-1-ol	430	(40)	213[4]	(91)			455.0[4]	(91)
2-methyl-2-penten-1-ol	441	(92)	199[4]	(91)	$7.44\ 10^{-4}$	(93)	455.8[4]	(91)
2-methylphenyl methanol	492	(92)	308	(88)			433.9[4]	(91)
4-ethyl phenyl methanol	389	(40)	358	(87)			405.7[4]	(91)
2,4,5-trimethyl phenyl methanol	562[4]	(91)	327[4]	(91)			391.5[4]	(91)
Ethyl heptanoate	461	(39)	207	(39)	$1.03\ 10^{-1}$ (20°C)	(96)	283.1[4]	(89)

[4] *calculated with Joback's method* (91)

4. Description of the literature studies concerning the combustion kinetics of oxygenated aromatics, which are the main components of EHL-derived fuels

Oxygenated aromatics are an important fraction of the bio-oil composition. These typical alternative fuels are derived by from EHL by the Chemical transformation of enzymatic hydrolysis lignin with catalytic solvolysis under mild conditions. Table 12 presents the aromatic oxygenates, for which kinetic studies are available. In our analysis, only work performed after 1980 was comprehensively considered.

Table 12: Structure of aromatic oxygenates, for which kinetic studies are available.

Chemical name	The structure
Phenol	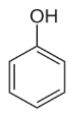
Anisole	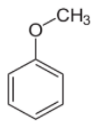
benzyl alcohol	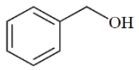
1 phenyl ethanol, 2 phenyl ethanol	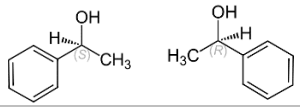
Catechol	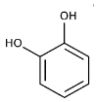
o, m, p-cresol	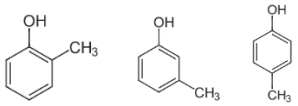
o-Guaiacol	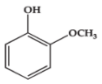

4.1. Phenol

Phenol is the lightest aromatic oxygenates. The kinetic studies related to its combustion are shown in Table 13. In 1988, He et *al*. (96) measured in a single-pulse shock tube the rate constants of the hydrogen atom and hydroxyl radical attack on phenol. Experiments were performed over a range of temperatures from 1000 to 1150 K and pressures from 2.5 to 5 atm. After that, Lovell et *al*. (97) studied the pyrolysis of phenol in the Princeton flow reactor at atmospheric pressure for temperature between 1064 and 1162 K. Using gas chromatography, they identified the main pyrolysis products, which are CO, cyclopentadiene and benzene.

Manion et *al*. (98) drew similar conclusions from their work on the phenol pyrolysis in H_2 also using a flow reactor over a temperature range (T = 922-1175 K). In line with their pyrolysis study, Brezinsky et *al*. (100) investigated the oxidation of phenol at atmospheric pressure near 1170 K over a range of equivalence ratios (ϕ), 0.64-1.73. They found that cyclopentadiene was the major reaction intermediate and proposed its formation to occur through that of cyclopentadienyl radical, which is produced via reaction (1).

$$C_6H_5O^* = CO + C_5H_5^* \text{ (reaction 1)}$$

Other observed major species included carbon monoxide carbon dioxide, acetylene, benzene, 1,3-butadiene, ethylene, and methane. Minor species were allene, methylacetylene, propene, ethane, methylcyclopentadiene, and naphthalene.

Horn et *al*. (99) studied the pyrolysis of phenol in a shock tube in a high temperature range from 1450 to 1650 K using atomic and molecular resonance absorption spectroscopy as diagnostics. They deduced from their results that the main initiation reaction is the elimination of CO after an internal rearrangement of phenol. No study on phenol flame could be found.

Table 13: Summary of the main experimental kinetic studies about phenol.

Instrument	Measured property	Experimental Conditions	Reference
Shock tube	Rate constant for H and OH H-abstraction	T=1000-1150 K; P=2.5-5 atm	He et al., 1988 (96)
Flow reactor	Species profiles	T=1064-1162 K; P=1 atm; Φ=∞	Lovell et *al*.,1989 (97)
		T=922-1175 K; P=1 atm; Φ=∞	Manion et *al*., 1989 (98)
Shock tube		T=1450-1650 K; P=2.5 atm; Φ=∞	Horn et *al*., 1998 (99)
		T=1170 K; P=1 atm; Φ=∞-0.64-1.73	Brezinsky et al., 1998 (100)

4.2. Anisole

Anisole is the aromatic oxygenate, whose combustion kinetics has been the mostly studied; as shown in Table 14. Its first pyrolysis study was performed in a stirred reactor by Mulcahy et al. (101) at low temperatures (453 and 539 K). In 1980, Schlosberg et *al*. (102) studied the pyrolysis of anisole in a batch reactor at a constant temperature of 723 K and at atmospheric pressure. Methane and CO were found to be the main products of this pyrolysis, the other detected products were H_2, water, phenol. Lin and Lin (103) studied for the first time the thermal decomposition of anisole in a shock tube. Experiments were performed between 1000 and 1580 K. The CO formed in the reaction was monitored by resonance-absorption using a stabilized CW CO laser allowing to propose rate constants for related reactions, especially that of reaction (1) of phenol.

Concerning anisole pyrolysis studies in flow reactors. Mackie et *al*. (104) studied its pyrolysis in a perfectly stirred reactor at low pressures (P=0.015-0.12 atm) and low temperatures (T=850-1000 K). They observed CO, phenol and cresols as the most important products. In 2001, Platonov et *al*. (105) used a flow reactor with gas chromatography and showed that increasing the temperature decreased the formation of phenolic compounds and increased that of PAHs. Friderichsen et *al*. 0 (107) also used a flow reactor, together with a hyperthermal nozzle; thanks to time-of-flight mass spectrometry and Fourier transform infrared spectroscopy, they identified free radicals and reaction intermediates and demonstrated the important role of phenoxy and cyclopentadienyl radicals in the formation of naphthalene. More recently, Pelucchi et *al*. (108) used a flow reactor to quantify products from anisole pyrolysis. The main stable products detected were CO, CH_4, C_2H_6, benzene and benzofuran.

The oxidation of anisole has been less studied than its pyrolysis. In 1997, Pecullan et *al*. (109) were the first to study the pyrolysis and oxidation of anisole. The experiments were carried out at high temperatures (T = 999-1003 K) and at atmospheric pressure in the Princeton flow reactor with gas chromatography analysis. Major products were phenol, cresols, methylcyclopentadiene, and CO; minor ones included benzene, cyclopentadiene, ethane, and methane.

More recently, the pyrolysis of anisole and its oxidation under stoichiometric oxidation were studied by Nowakowska et *al*. 0 in a jet-stirred reactor. The main reaction products were measured by gas chromatography versus temperature Major products were methane, carbon monoxide, benzene, phenol and hydrogen; minor ones included benzofuran, xylenes, styrene, and naphthalene. Finally, Wagnon et *al*. (46) conducted an experimental study on the pyrolysis and the oxidation of anisole in a jet-stirred reactor in the temperature range 675–1275K, at 1 atm and at equivalence ratios of 0.5, 1 and 2. Major products were CO, 1,3-cyclopentadiene, benzene, cresols; minor ones included toluene, styrene, ethane, and methane.

A few studies in flame were made with anisole. The first laminar flame speed measurements of anisole were performed in 2017. Wu et *al*. (111) used OH chemiluminescence on a Bunsen burner for various equivalence ratios and different pressures. Wagnon et *al*. (46) also measured burning velocities thanks to the heat flux method on a flat flame burner at 358 K and ambient pressure. In 2019, Zare et *al*. (112) completed flame speed measurement with the bomb method at temperatures from 460 to 575K and pressures from 0.5 to 3 atm.

Concerning product measurements in anisole flames, in 2019, Bierkandt et *al.* (113) published flame structures at two equivalence ratios, 1.2 and 1.6. Products measurements were performed by photoionization mass spectrometry and photoelectron spectroscopy. In addition to CO and H_2, the

intermediates produce in the highest amounts, with mole fractions on the order of 10^{-3} –10^{-2}, were methyl radical (CH_3), CH_4, C_2H_2, C_2H_4, C_2H_6, CH_2O, cyclopentadienyl radical (C_5H_5), cyclopentadiene (C_5H_6), benzene (C_6H_6), phenol (C_6H_5OH), and benzaldehyde (C_6H_5CHO).

Table 14: Summary of the main experimental studies about anisole.

Instrument	Measured property	Experimental Conditions	Reference
Batch reactor	Species profiles	T=723 K; P=1 atm; Φ=∞	Schlosberg et *al*., 1983 (102)
Shock tube		T=1000-1580 K; P=0.4-0.9 atm; Φ=∞	Lin and Lin., 1986 (103)
Perfectly-stirred reactor		T=850-1000 K; P=0.015-0.12atm; Φ=∞	Mackie et *al*., 1990 (104)
		T=673-1173 K; P=1 atm; Φ=∞,1	Nowakowska et *al,* (110)
		T=675-1275 K; P=1 atm; Φ=∞, 0.5, 1 and 2.	Wagnon et *al*., 2018 (46)
Flow reactor		T=1023-1173 K; Φ=∞	Platonov et *al*., 2001 (105)
		T=793-1020 K; P=1 atm; Φ=∞	Arends et al., 1993 (106)
		T=873-1373 K; P=1 atm; Φ=∞	Friderichsen et *al*., 02001 (107)
		T= 525-675 K; P=1 atm; Φ=∞	Pelucchi et al. 2018 (108)
		T=999-1003 K; P=1 atm; Φ=∞, 1.05, 0.62,1.71	Pecullan et *al*., 1997 (109)
Bunsen burner	Laminar flame speed	T=423 K; P=1-7.5 bar; Φ=0.75 T=423 K; P=1 bar; Φ=0.6-1.3	Wu et *al*., 2017 (111)
Flat flame burner		T=358 K; P=1 atm; Φ=0.6-1.2	Wagnon et *al*., 2018 (46)
Constant Volume Chamber		T=460-575 K; P=1atm; Φ=0.8-1.4 T=460-575 K; P=0.5-3 atm; Φ=1	Zare et *al*., 2019 (112)
Burner	Product and temperature flame structure	T=500 K; P=0.04 bar; Φ=1.2,1.6	Bierkandt et *al*., 2019 (113)

4.3. Benzyl alcohol

Only one kinetic study concerning benzyl alcohol was found. Zhou et *al.* (114) studied the oxidation of benzyl alcohol in an atmospheric jet-stirred reactor with gas chromatography analysis at equivalence

ratios, 0.4 and 2.0, at temperature between 700–1100 K; 19 species were detected, including fuel. Major products were benzene, benzaldehyde, and CO; minor ones included acetaldehyde, phenol, benzofuran, ethane, and methane. No study on benzyl alcohol flame could be found.

Table 15: Summary of the main experimental studies about benzyl alcohol.

Instrument	Measured property	Experimental conditions	Reference
Jet-stirred reactor	Species profiles	T=700–1100 K; P=1 atm; Φ=0.4, and 2.0.	Zhou et al., 2018 (114)

4.4. Phenyl-ethanols

Several gas-phase kinetic studies were recently performed with 2-phenyl-ethanol because of its strong ignition resistance and its high heating value compared to other oxygenated aromatics. The first kinetic experiments concerned its pyrolysis in a closed static reactor by Taylor et *al*. (115) in 1988 (T=720-767 K, P = 1 bar) and Chuchani et *al*. in 1999 (116) (T=743-1040 K, P=65-198 Torr). They both observed the same major produced species, styrene and toluene, and ethylbenzene as a minor one; Taylor also found traces of biphenyl, bibenzyl, 2-methoxyethylbenzene and 2-phenylethylether.

In 2017, Kiran et *al*. (118) pyrolyzed 2-phenyl-ethanol in a shock tube at pressures from 7 to 13 atm and for temperatures from 1011 to 1446 K. The main products were styrene, benzene and toluene, with ethylbenzene and phenylacetylene found in smaller quantities and benzaldehyde observed as traces.

In 2021, Brian et *al*. (117) measured the tendency of 1- and 2- phenyl-ethanol to produce soot during their oxidation in an isothermal flow reactor at temperatures from 800 to 1200 K and atmospheric pressure. Using gas chromatography, for the chosen rich mixture (Φ=3), they found carbon monoxide, benzene, styrene, toluene and benzaldehyde to be the main products; the formation of acetophenone was also reported for 1-phenyl-ethanol and that of phenylacetaldehyde for 2-phenyl-ethanol.

In 2017, Shankar et *al*. (119) used a shock tube to measure the ignition delay times of 2-phenyl-ethanol at 10 and 20 bar, for two equivalence ratios (0.5 and 1) and for temperatures from 1050 to 1500 K. Fang et *al*. (120) also evaluated the ignition delay times of 2-phenyl-ethanol. They used a rapid compression machine at pressures from 10 to 40 bar, temperatures from 813 to 992 K and for equivalence ratios between 0.35 and 1.5.

No study on phenyl-ethanol flame could be found.

Table 16: Summary of the main experimental studies about phenyl-ethanol.

Instrument	Measured property	Experimental conditions	Reference
Closed vessel	Species profiles	T=720-767 K; P = 1 bar; Φ=∞	Taylor et al., 1988 (115)
		T=743-1040 K; P=0.086-0.263bar; Φ=∞	Chuchani et al., 1999 (116)
Plug Flow Reactor		T=800-1200 K; Φ=3	Brian et al., 2021 (117)
Shock Tube		T= 1011-1446 K; P=7-13 atm; Φ=∞	Kiran et al., 2017 (2017)
	Ignition delay times	T=1050-1500 K; P=10 and 20 bar; Φ=0.5 and 1	Shankar et al., 2017 (119)
Rapid Compression Machine		T=813-992 K; P=10-40 bar; Φ=0.35 and 1.5	Fang et al., 2021 (120)

4.5. Catechol

Catechol is a phenol-type compound representative of the structural entities of biomass, charcoal and wood. Table 17 shows the main combustion kinetics studies related to catechol. In 2002, Wornat et *al.* (121) studied the pyrolysis of catechol in a flow reactor at a temperature of 1273 K, at atmospheric pressure. They used high pressure liquid chromatography with detection by UV-visible diode (UV) to identify 59 species. The same team (122) repeated the same study at lower temperature, from 973 K, with gas chromatography quantification. The main products obtained were CO, acetylene, 1,3-butadiene, phenol, cyclopentadiene, benzene and ethylene; minor products were methane, ethane, propyne, propadiene, and propylene.

Again, in the same team, Thomas et *al.* (123) investigated the gas-phase pyrolysis and oxidation of catechol with equivalence ratios ranging from ∞ (pure pyrolysis) to 1.08 (near stoichiometric oxidation). Experiments were conducted over a temperature range of 500–1000 °C. Major products were CO, acetylene, phenol, benzene, vinylacetylene, ethylene, methane, cyclopentadiene, styrene, and phenylacetylene; minor ones included ethane, propyne, propadiene, propylene and toluene.

No study on catechol flame could be found.

Table 17: Summary of the main experimental studies about catechol.

Instrument	Measured property	Experimental Conditions	Reference
Flow reactor	Species profiles	T=973,15-1273 K; P=1 atm; Φ=∞	Wornat et *al.*, 2002 (122)
		T=773-1273 K; P=1 atm; Φ=0-0.92	Thomas et *al.*, 2007 (123)

4.6. Cresols

No study could be found on cresol gas phase kinetics. The only cresol kinetic studies were performed by Martino et *al.* (124, 125) in supercritical water solution in a flow reactor. The oxidation of o-cresol was studied at pressures 200-300 atm, temperatures 623-773 K and lean equivalence ratios (0.0285-0.524) (124). Except carbon dioxide and carbon monoxide, the main products were phenol, 2-hydroxybenzaldehyde, benzodioxole and indanone. The same team (125) studied the thermal decomposition of o-, m- and p-cresols in supercritical water at 733 K and 250 atm. A very poor conversion was observed, with nevertheless the reported formation of phenol and of the corresponding o-, m- or p-hydroxybenzaldehydes.

4.7. Guaiacol

Guaiacol is a low molecular weight semi-volatile polar aromatic compound, and one of the main primary tars produced during lignin pyrolysis. Its combustion kinetics studies are presented in Table 18. Guaiacol reactions were first investigated in closed vessels. In 1963, Klein et *al*. (126) investigated its thermal decomposition at atmospheric pressure for temperatures ranging from 523 to 873 K. They detected at low conversion methane, carbon monoxide, pyrocatechol and phenol as the only products. In 1982, Ceylan et *al*. (127) studied the thermolysis of guaiacol in tetralin, at 578-618 K and mostly found the formation of phenol, o-cresol, methylcatechols, and methylguaiacols.

Concerning flowing experiments, Scheer et *al.* **Error! Reference source not found.** used a heated SiC micro tubular (µ-tubular) reactor at low-pressure to investigate the pyrolysis of guaiacol at high temperature, up to 1575 K. The decomposition products were detected by both photoionization time-of-flight mass spectroscopy and infrared spectroscopy). They reported to formation of CO, phenol, cyclopentadione.

More recently, guaiacol pyrolysis and oxidation was studied by Nowakowska et *al.* (129) under stoichiometric conditions in a jet stirred reactor between 623 and 923 K for a residence time of 2 s. The main primary products were CO, acetylene, benzene, and phenolic molecules as pyrocatechol and methylcatechols; minor ones included ethane, propyne, propadiene, anisole and toluene.

No study on catechol flame could be found.

Table 18: Summary of the main experimental studies about guaiacol.

Instrument	Measured property	Experimental conditions	Reference
Closed vessel	Species profiles	T=623-923 K; P=1 atm; Φ=∞	Klein et *al*., 1963 (126)
		T=578-618 K; P=1atm	Ceylan et *al*., 1982 (127)
Jet-stirred reactor		T=623-923 K; P=1 atm; t=2s	Nowakowska et *al.*, 2014 (129)

4.8. Summary of species produced during the oxidation of oxygenated aromatics

Table 19 summarizes the products which were reported during the kinetic investigations of the oxidation of the oxygenated aromatics listed in Table 12. As they are the products of the complete combustion, H_2O and CO_2 are not specified in Table 19, their presence is implicit. No gas-phase study was found for cresol.

CO was reported as the major product from all the investigated reactants, with the kinetic importance of reaction (1) underlined in most the studies. A significant formation of benzene can also be noted due to the easy ipso-addition of H-atoms, see reaction (2) in the case of phenol:

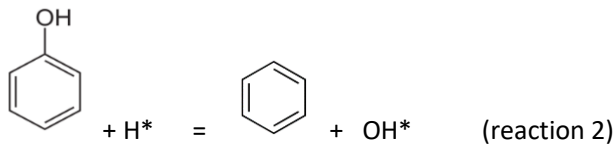

(reaction 2)

Two usual soot precursors, naphthalene and 1,3-cyclopentadiene, are also often reported, it is also the case for acrolein, a toxic aldehyde.

Table 19: Products species of kinetics experiments in past oxidation studies.

	Major species (>10%)	**Minor species (<10%)**	
		Non-aromatic	**Aromatic**
Phenol	CO, 1,3-Cyclopentadiene, Benzene.	allene, methylacetylene, propene, ethane, methylcyclopentadiene.	Naphthalene.
Anisole	CO, Acetylene, Propene, Acetaldehyde,1,3-Cyclopentadiene, Benzene, Cresols.	Methane, Ethylene, Allene, Propyne, 1-Butyne, Acrolein, 1,3-Pentadiene.	Fulvene, Toluene, Phenol, Styrene, Guaiacol Ethylbenzene, Indene, Benzofuran, Naphthalene, dihydronaphthalene,
Benzyl alcohol	CO, Methane, Ethylene, Benzene, Phenol, Benzaldehyde.	Ethane, Propylene, butane, Acetaldehyde, Acrolein.	Benzofuran, Benzyl formate, benzyl acetate and benzyl propionate
Phenyl ethanols	CO, Styrene, Benzene, Toluene		Ethylbenzene, Phenylacetylene, Benzaldehyde, acetophenone and phenyl-acetaldehyde.
Catechol	CO, Methane, Ethylene, Benzene.	Propene, Propadiene, Acetylene, Phenylacetylene, Vinylacetylene, 1,3-Cyclopentadiene,	Styrene, Toluene
Guaiacol	CO, Methane, Benzene, Phenol, Cresols, Pyrocatechol.	Acetylene, Ethylene, Ethane, Methanol, Acetaldehyde, Acrolein	Benzaldehyde, Anisole, 2-Hydroxybenzaldehyde.

4.9. Conclusion for this part

This bibliographic review showed that the literature is poor as far as phenolic compound gas phase oxidation is concerned. This is due to experimental difficulties in handling these species due to their low volatility. Most of them are even solid at room temperature. This is the case of phenol, the phenolic compound with the simplest structure (boiling point of 455 K at atmospheric pressure, see Table 5). As a matter of fact, studies mainly concern anisole and guaiacol, and there is clearly a need of new data sets for better understanding the oxidation chemistry of these species.

The analysis of oxidation reaction products (see Table 19 for a summary) shows that phenolic compounds, depending on conditions, may lead to the formation of aromatic and poly aromatic hydrocarbons, and to that of unsaturated hydrocarbons. But again, very little literature studies report comprehensive intermediate mole fraction data sets and sometimes only for a few operating conditions.

As far as global reactivity indicators are concerned, there is also a lack of data. Ignition delay times and laminar urning velocities have been measured for very few species only. Table 20 summarizes experimental data types available for the phenolic compounds. Thus, new sets of experimental data are highly needed to better characterize the reactivity of this class of compounds.

Table 20: Map of available experimental data types for phenolic compounds.

	Detailed speciation	**Ignition delay times**	**Laminar burning velocities**
Phenol	X	**X**	0
Anisole	X	0	**X**
Benzyl alcohol	X	0	0
Phenyl ethanols	X	**X**	0
Catechol	X	0	0
Cresols	0	0	0
Guaiacol	X	0	0

5. Conclusion

To understand the purpose of valuing EHL, a large number of studies have been carried out in recent years to produce high performance fuel blends, i.e., high heating value jet-fuel, from technical lignins including EHL. However, understating of EHL structure and its exploitation towards added-value products are still needed urgently. For this, the project EHLCATHOL aims at developing a novel technology that fully takes the advantage and utilizes the energy of the waste-EHL by transforming it to high quality applicable liquid fuels. Oxygenated aromatics and alcohols constitute an important fraction of the composition of bio-oils obtained by valorization of EHL; arenes or solvents-derived-molecules are also existed in EHL-derived biofuel.

About the combustion properties of surrogates and catalysis solvents, auto-ignition, phase change state global fuel parameters are presented. About characteristic fuel data:

- LHV of arenes is close to that of traditional gasoline (≈ 42 MJ/kg). Concerning surrogate compounds and solvents, heating values are higher than that of ethanol (≈ 27 MJ/kg) but lower than that of existing bio-diesels (≈ 37 MJ/kg). So, at first sight, a biofuel composed of these species would have a LHV close to existing biofuels. A minimum value of 35 is needed in Europe for biodiesel (EN ISO 14214, (94)).

- Research Octane Numbers are, most of time, higher than the minimum value of 95 fixed by EN ISO 4259:2006 (95), so it is also expected for the final biofuel.

- Only a few of these molecules have higher Cetane Numbers than the minimum value of 51 fixed for biodiesel (EN ISO 14214 (94)) and diesel (EN ISO 4259:2006 (95)); therefore, at that moment, it might be difficult to use this kind of pure biofuel as biodiesel.

Kinetic studies on oxygenated aromatics expected in the composition of biofuels derived from lignin are also presented. Except for anisole, there is very little work on these species; this is mainly due to experimental difficulties related to the very low volatility of this class of compounds. Even if speciation data are available for some of them, it is only for a limited range of conditions. The lack of data is even more important for global reactivity indicators such as laminar burning velocities. Thus, new experimental studies are needed in order to better understand the combustion properties of these aromatic oxygenated fuels.

The objective is now to carry out additional studies on fuels resulting from the compounds of EHL solvolysis oil in order to better understand the specificities of this class of compounds (data speciation and laminar burning velocity measurements) and to develop a detailed kinetic model, permitting then the development of reliable bio-oil surrogates.

References

1. Wu X, Luo N, Xie S, Zhang H, Zhang Q, Wang F, et al. Photocatalytic transformations of lignocellulosic biomass into chemicals. Chem Soc Rev. 2020 Sep 1;49(17):6198–223.

2. Liu W-J, Li W-W, Jiang H, Yu H-Q. Fates of Chemical Elements in Biomass during Its Pyrolysis. Chem Rev. 2017 May 10;117(9):6367–98.

3. Chirat C. Use of vegetal biomass for biofuels and bioenergy. Competition with the production of bioproducts and materials? Comptes Rendus Physique. 2017 Sep 1;18(7):462–8.

4. Alaimo P, Langenhan J, Tanner M. 12. Chem. Eur. J. 2010, 16, 4970-4980. 2013.

5. Singh MK, Reddy KPJ, Arunan E. Shock Tube Experimental and Theoretical Study on the Thermal Decomposition of 2-Phenylethanol. In: Ben-Dor G, Sadot O, Igra O, editors. 30th International Symposium on Shock Waves 1. Cham: Springer International Publishing; 2017. p. 317–20.

6. Jung KA, Woo SH, Lim S-R, Park JM. Pyrolytic production of phenolic compounds from the lignin residues of bioethanol processes. Chemical Engineering Journal. 2015 Jan 1;259:107–16.

7. Diehl BG, Brown NR, Frantz CW, Lumadue MR, Cannon F. Effects of pyrolysis temperature on the chemical composition of refined softwood and hardwood lignins. Carbon. 2013 Aug 1;60:531–7.

8. Sain M, Panthapulakkal S. Bioprocess preparation of wheat straw fibers and their characterization. Industrial Crops and Products. 2006 Jan 1;23(1):1–8.

9. Shao L, Zhang X, Chen F, Xu F. Fast pyrolysis of Kraft lignins fractionated by ultrafiltration. Journal of Analytical and Applied Pyrolysis. 2017 Nov 1;128:27–34.

10. Valdivia M, Galan JL, Laffarga J, Ramos J-L. Biofuels 2020: Biorefineries based on lignocellulosic materials. Microbial Biotechnology. 2016;9(5):585–94.

11. Jin Y, Ruan X, Cheng X, Lü Q. Liquefaction of lignin by polyethyleneglycol and glycerol. Bioresource Technology. 2011 Feb 1;102(3):3581–3.

12. Zhang B, Yang D, Wang H, Qian Y, Huang J, Yu L, et al. Activation of Enzymatic Hydrolysis Lignin by NaOH/Urea Aqueous Solution for Enhancing Its Sulfomethylation Reactivity. ACS Sustainable Chem Eng. 2019 Jan 7;7(1):1120–8.

13. (a) Xie D, Si C, Huo D. Enzymatic Hydrolysis Lignin (EHL) and its applications for value-added products, a quick review. J Bioresour Bioprod. 2017;2(4):163–9; (b) M. Yu. Balakshin Et al. New Opportunities in the Valorization of Technical Lignins. ChemSusChem 2021, 14, 1016 –36.

14. Cheng, Liu X S. Research progress of enzymatic hydrolysis lignin and its application in rubber industry. Rubber technology market. 2009;23–6.

15. Cheng, T. Modification of alkali lignin and its surface activity study [Internet]. 2013. Available from: Master Degree Dissertation Submitted to Southeast University.

16. LI H, DENG Y-H, ZHANG X-H, QIU X-Q. Influence of Temperature on Microstructure and Physicochemical Properties of Alkali Lignin in Aqueous Solution. Acta Physico-Chimica Sinica. 2015 Jun 15;31(6):1118–28.

17. Mo X. Reinforcing properties of enzymatic hydrolysis lignin for acrylonitrile butadiene rubber. 2013.

18. Lawther JM, Sun R. The fractional characterisation of polysaccharides and lignin components in alkaline treated and atmospheric refined wheat straw. Industrial Crops and Products. 1996 Jun 1;5(2):87–95.

19. de Wild P, Van der Laan R, Kloekhorst A, Heeres E. Lignin valorisation for chemicals and (transportation) fuels via (catalytic) pyrolysis and hydrodeoxygenation. Environmental Progress & Sustainable Energy. 2009;28(3):461–9.

20. Barta K, Matson TD, Fettig ML, Scott SL, Iretskii AV, Ford PC. Catalytic disassembly of an organosolv lignin via hydrogen transfer from supercritical methanol. Green Chem. 2010 Sep 3;12(9):1640–7.

21. Catalytic Lignin Valorization Process for the Production of Aromatic Chemicals and Hydrogen - Zakzeski - 2012 - ChemSusChem - Wiley Online Library [Internet]. [cited 2021 Sep 30]. Available from: https://chemistry-europe.onlinelibrary.wiley.com/doi/abs/10.1002/cssc.201100699

22. Jongerius AL, Bruijnincx PCA, Weckhuysen BM. Liquid-phase reforming and hydrodeoxygenation as a two-step route to aromatics from lignin. Green Chem. 2013 Oct 22;15(11):3049–56.

23. Huang X, Korányi TI, Boot MD, Hensen EJM. Catalytic Depolymerization of Lignin in Supercritical Ethanol. ChemSusChem. 2014;7(8):2276–88.

24. Catalytic Ethanolysis of Kraft Lignin into High-Value Small-Molecular Chemicals over a Nanostructured α-Molybdenum Carbide Catalyst - Ma - 2014 - Angewandte Chemie - Wiley Online Library [Internet]. [cited 2021 Sep 30]. Available from: https://onlinelibrary.wiley.com/doi/abs/10.1002/ange.201402752

25. Ma X, Ma R, Hao W, Chen M, Yan F, Cui K, et al. Common Pathways in Ethanolysis of Kraft Lignin to Platform Chemicals over Molybdenum-Based Catalysts. ACS Catal. 2015 Aug 7;5(8):4803–13.

26. Chen M, Hao W, Ma R, Ma X, Yang L, Yan F, et al. Catalytic ethanolysis of Kraft lignin to small-molecular liquid products over an alumina supported molybdenum nitride catalyst. Catalysis Today. 2017 Dec 1;298:9–15.

27. Yan F, Ma R, Ma X, Cui K, Wu K, Chen M, et al. Ethanolysis of Kraft lignin to platform chemicals on a MoC1-x/Cu-MgAlOz catalyst. Applied Catalysis B: Environmental. 2017 Mar 1;202:305–13.

28. Huang X, Atay C, Korányi TI, Boot MD, Hensen EJM. Role of Cu–Mg–Al Mixed Oxide Catalysts in Lignin Depolymerization in Supercritical Ethanol. ACS Catal. 2015 Dec 4;5(12):7359–70.

29. Chesi C, de Castro IBD, Clough MT, Ferrini P, Rinaldi R. The Influence of Hemicellulose Sugars on Product Distribution of Early-Stage Conversion of Lignin Oligomers Catalysed by Raney Nickel. ChemCatChem. 2016;8(12):2079–88.

30. Bosch SV den, Renders T, Kennis S, Koelewijn S-F, Bossche GV den, Vangeel T, et al. Integrating lignin valorization and bio-ethanol production: on the role of Ni-Al2O3 catalyst pellets during lignin-first fractionation. Green Chem. 2017 Jul 17;19(14):3313–26.

31. Korányi TI, Huang X, Coumans AE, Hensen EJM. Synergy in Lignin Upgrading by a Combination of Cu-Based Mixed Oxide and Ni-Phosphide Catalysts in Supercritical Ethanol. ACS Sustainable Chem Eng. 2017 Apr 3;5(4):3535–43.

32. Tymchyshyn M, Yuan Z, Zhang Y, Xu CC. Catalytic hydrodeoxygenation of guaiacol for organosolv lignin depolymerization – Catalyst screening and experimental validation. Fuel. 2019 Oct 15;254:115664.

33. Qin S, Li B, Luo Z, Zhao C. The conversion of a high concentration of lignin to cyclic alkanes by introducing Pt/HAP into a Ni/ASA catalyst. Green Chem. 2020 May 11;22(9):2901–8.

34. Wang S, Gao W, Xiao L-P, Shi J, Sun R-C, Song G. Hydrogenolysis of biorefinery corncob lignin into aromatic phenols over activated carbon-supported nickel. Sustainable Energy Fuels. 2019 Jan 29;3(2):401–8.

35. Bai Y, Cui K, Sang Y, Wu K, Yan F, Mai F, et al. Catalytic Depolymerization of a Lignin-Rich Corncob Residue into Aromatics in Supercritical Ethanol over an Alumina-Supported NiMo Alloy Catalyst. Energy Fuels. 2019 Sep 19;33(9):8657–65.

36. Mai F, Wen Z, Bai Y, Ma Z, Cui K, Wu K, et al. Selective Conversion of Enzymatic Hydrolysis Lignin into Alkylphenols in Supercritical Ethanol over a WO3/γ-Al2O3 Catalyst. Ind Eng Chem Res. 2019 Jun 19;58(24):10255–63.

37. Sang Y, Chen M, Yan F, Wu K, Bai Y, Liu Q, et al. Catalytic Depolymerization of Enzymatic Hydrolysis Lignin into Monomers over an Unsupported Nickel Catalyst in Supercritical Ethanol. Ind Eng Chem Res. 2020 Apr 22;59(16):7466–74.

38. Tymchyshyn M, Rezayan A, Yuan Z, Zhang Y, Xu CC. Reductive hydroprocessing of hydrolysis lignin over efficient bimetallic catalyst MoRu/AC. Industrial & Engineering Chemistry Research. 2020;59(39):17239–49.

39. FLUIDAT® on the Net, mass flow and physical properties calculations [Internet]. [cited 2021 Sep 28]. Available from: https://www.fluidat.com/default.asp

40. Informatics NO of D and. WebBook de Chimie NIST [Internet]. National Institute of Standards and Technology; [cited 2021 Sep 28]. Available from: https://webbook.nist.gov/chemistry/

41. Tian M, McCormick RL, Ratcliff MA, Luecke J, Yanowitz J, Glaude P-A, et al. Performance of lignin derived compounds as octane boosters. Fuel. 2017 Feb 1;189:284–92.

42. McCormick RL, Ratcliff MA, Christensen E, Fouts L, Luecke J, Chupka GM, et al. Properties of Oxygenates Found in Upgraded Biomass Pyrolysis Oil as Components of Spark and Compression Ignition Engine Fuels. Energy Fuels. 2015 Apr 16;29(4):2453–61.

43. Zhou L, Boot MD, Johansson BH, Reijnders JJE. Performance of lignin derived aromatic oxygenates in a heavy-duty diesel engine. Fuel. 2014 Jan 1;115:469–78.

44. Tian M. Lignocellulosic octane boosters. Technische Universiteit Eindhoven; 2016.

45. Schweidtmann AM, Rittig JG, König A, Grohe M, Mitsos A, Dahmen M. Graph Neural Networks for Prediction of Fuel Ignition Quality. Energy Fuels. 2020 Sep 17;34(9):11395–407.

46. Wagnon SW, Thion S, Nilsson EJK, Mehl M, Serinyel Z, Zhang K, et al. Experimental and modeling studies of a biofuel surrogate compound: laminar burning velocities and jet-stirred reactor measurements of anisole. Combustion and Flame. 2018 Mar 1;189:325–36.

47. McCormick RL, Fioroni G, Fouts L, Christensen E, Yanowitz J, Polikarpov E, et al. Selection Criteria and Screening of Potential Biomass-Derived Streams as Fuel Blendstocks for Advanced Spark-Ignition Engines. SAE International Journal of Fuels and Lubricants. 2017;10(2):442–60.

48. Ratcliff MA, Burton J, Sindler P, Christensen E, Fouts L, Chupka GM, et al. Knock Resistance and Fine Particle Emissions for Several Biomass-Derived Oxygenates in a Direct-Injection Spark-Ignition Engine. SAE International Journal of Fuels and Lubricants. 2016;9(1):59–70.

49. Szybist JP, Splitter DA. Understanding chemistry-specific fuel differences at a constant RON in a boosted SI engine. Fuel. 2018 Apr 1;217:370–81.

50. Zhou L, Boot MD, Goey LPH de. Gasoline - Ignition Improver - Oxygenate Blends as Fuels for Advanced Compression Ignition Combustion [Internet]. Warrendale, PA: SAE International; 2013 Apr [cited 2021 Sep 28]. Report No.: 2013-01–0529. Available from: https://www.sae.org/publications/technical-papers/content/2013-01-0529/

51. Wu Y, Apeloig J, Rouet E, Rossow B, Modica V, Barviau B, et al. MESURE DE LA VITESSE DE FLAMME LAMINAIRE DE COMPOSÉS HYDROCARBONÉS OXYGÉNÉS PURS ET DE BIOCARBURANTS DÉRIVÉS DE LA BIOMASSE LIGNOCELLULOSIQUE CONTENANT DES COMPOSÉS OXYGÉNÉS. :10.

52. Zhou L, Heuser B, Boot M, Kremer F, Pischinger S. Performance and Emissions of Lignin and Cellulose Based Oxygenated Fuels in a Compression-Ignition Engine [Internet]. Warrendale, PA: SAE International; 2015 Apr [cited 2021 Sep 28]. Report No.: 2015-01–0910. Available from: https://www.sae.org/publications/technical-papers/content/2015-01-0910/

53. Cox JD. The heats of combustion of phenol and the three cresols. Pure and Applied Chemistry. 1961 Jan 1;2(1–2):125–8.

54. Bhatia SK, Gurav R, Choi T-R, Han YH, Park Y-L, Park JY, et al. Bioconversion of barley straw lignin into biodiesel using Rhodococcus sp. YHY01. Bioresource Technology. 2019 Oct 1;289:121704.

55. Gouvernement du Canada E et C climatique C. ARCHIVÉE - Environnement et Changement climatique Canada - Rapport d'évaluation pour Pyrocatéchol [Internet]. 2010 [cited 2021 Sep 28]. Available from: https://www.ec.gc.ca/ese-ees/default.asp?lang=Fr&n=04FDC10E-1#a4

56. Knop V, Loos M, Pera C, Jeuland N. A linear-by-mole blending rule for octane numbers of n-heptane/iso-octane/toluene mixtures. Fuel. 2014 Jan 1;115:666–73.

57. Shankar VSB, Al-Abbad M, El-Rachidi M, Mohamed SY, Singh E, Wang Z, et al. Antiknock quality and ignition kinetics of 2-phenylethanol, a novel lignocellulosic octane booster. Proceedings of the Combustion Institute. 2017 Jan 1;36(3):3515–22.

58. Pan M, Wei H, Feng D, Pan J, Huang R, Liao J. Experimental study on combustion characteristics and emission performance of 2-phenylethanol addition in a downsized gasoline engine. Energy. 2018 Nov 15;163:894–904.

59. Pouvoir calorifique. In: Wikipédia [Internet]. 2021 [cited 2021 Sep 28]. Available from: https://fr.wikipedia.org/w/index.php?title=Pouvoir_calorifique&oldid=180563458

60. Heating Value of Natural Gas & for other hydrocarbons [Internet]. EnggCyclopedia. 2011 [cited 2021 Sep 28]. Available from: https://www.enggcyclopedia.com/2011/09/heating-values-natural-gas/

61. Jones DSJ, Pujadó PP. Handbook of Petroleum Processing. Springer Science & Business Media; 2006. 1357 p.

62. Morgan N, Smallbone A, Bhave A, Kraft M, Cracknell R, Kalghatgi G. Mapping surrogate gasoline compositions into RON/MON space. Combustion and Flame. 2010 Jun 1;157(6):1122–31.

63. Jameel A, Gani A. A functional group approach for predicting fuel properties. 2019 Mar [cited 2021 Sep 28]; Available from: https://repository.kaust.edu.sa/handle/10754/631722

64. Silva G da, Bozzelli JW. On the reactivity of methylbenzenes. Combustion and Flame. 2010 Nov 1;157(11):2175–83.

65. Foong TM, Morganti KJ, Brear MJ, da Silva G, Yang Y, Dryer FL. The octane numbers of ethanol blended with gasoline and its surrogates. Fuel. 2014 Jan 1;115:727–39.

66. Yanowitz J, Ratcliff MA, McCormick RL, Taylor JD, Murphy MJ. Compendium of Experimental Cetane Numbers [Internet]. National Renewable Energy Lab. (NREL), Golden, CO (United States); 2017 Feb [cited 2021 Sep 28]. Report No.: NREL/TP-5400-67585. Available from: https://www.osti.gov/biblio/1345058

67. Garg SK, Banipal TS, Ahluwalia JC. Heat capacities and densities of liquid o-xylene, m-xylene, p-xylene, and ethylbenzene, at temperatures from 318.15 K to 373.15 K and at pressures up to 10 MPa. The Journal of Chemical Thermodynamics. 1993 Jan 1;25(1):57–62.

68. Verevkin SP. Thermochemical investigation on α-methyl-styrene and parent phenyl substituted alkenes. Thermochimica Acta. 1999 Feb 8;326(1):17–25.

69. Heating values of hydrogen and fuels [Internet]. [cited 2021 Sep 28]. Available from: https://chemeng.queensu.ca/courses/CHEE332/files/ethanol_heating-values.pdf

70. An experimental study on using diethyl ether in a diesel engine operated with diesel-biodiesel fuel blend | Elsevier Enhanced Reader [Internet]. [cited 2021 Sep 29]. Available from: https://reader.elsevier.com/reader/sd/pii/S2215098617317858?token=C0D07FAB86C62C1819B35696736859051BAD0EDCD609448B71669CD3293811402AF1D8C42BC59149D48FBBE5AF77FAC3&originRegion=eu-west-1&originCreation=20210929131428

71. McCormick R (ORCID:0000000314627165), Ratcliff M (ORCID:0000000156163317), Zigler B (ORCID:0000000215465025), Farrell J. Bioblendstocks that Enable High Efficiency Engine Designs [Internet]. National Renewable Energy Lab. (NREL), Golden, CO (United States); 2016 Dec [cited 2021 Sep 28]. Report No.: NREL/PR-5400-67629. Available from: https://www.osti.gov/biblio/1337921

72. McAllister S, Chen J-Y, Fernandez-Pello AC. Fundamentals of Combustion Processes. In: McAllister S, Chen J-Y, Fernandez-Pello AC, editors. Fundamentals of Combustion Processes [Internet]. New York, NY: Springer; 2011 [cited 2021 Sep 28]. p. 1–302. (Mechanical Engineering Series). Available from: https://doi.org/10.1007/978-1-4419-7943-8_9

73. LowerHeatingValue [Internet]. [cited 2021 Sep 28]. Available from: https://fchartsoftware.com/ees/eeshelp/hs706.htm

74. Howard MS, Issayev G, Naser N, Sarathy SM, Farooq A, Dooley S. Ethanolic gasoline, a lignocellulosic advanced biofuel. Sustainable Energy Fuels. 2019 Jan 29;3(2):409–21.

75. Kharitonov AS, Ivanov DP, Parfenov MV, Piryutko LV, Semikolenov SV, Dubkov KA, et al. New methods for the preparation of high-octane components from catalytic cracking olefins. Catal Ind. 2017 Jul 1;9(3):204–11.

76. Chen H, Zhou Z, He J, Zhang P, Zhao X. Effect of isopropanol and n-pentanol addition in diesel on the combustion and emission of a common rail diesel engine under pilot plus main injection strategy. Energy Reports. 2020 Nov 1;6:1734–47.

77. Han J, Somers LMT. Comparative investigation of ignition behavior of butanol isomers using constant volume combustion chamber under diesel-engine like conditions. Fuel. 2021 Nov 15;304:121347.

78. Pfromm PH, Amanor-Boadu V, Nelson R, Vadlani P, Madl R. Bio-butanol vs. bio-ethanol: A technical and economic assessment for corn and switchgrass fermented by yeast or Clostridium acetobutylicum. Biomass and Bioenergy. 2010 Apr 1;34(4):515–24.

79. Ganapathy V. DESIGN AND DEVELOPMENT OF STIRLING ENGINE CAR. 2015.

80. Yang C, Liu H, He K, Xue Y, Li Y, Chang X, et al. Effects of cetane number improvers on diesel fuel from direct coal liquefaction. Energy Sources, Part A: Recovery, Utilization, and Environmental Effects. 2016 Nov 1;38(21):3207–13.

81. Penner D, Redepenning C, Mitsos A, Viell J. Conceptual Design of Methyl Ethyl Ketone Production via 2,3-Butanediol for Fuels and Chemicals. Ind Eng Chem Res. 2017 Apr 12;56(14):3947–57.

82. Kessler T, Sacia ER, Bell AT, Mack JH. Artificial neural network based predictions of cetane number for furanic biofuel additives. Fuel. 2017 Oct 15;206:171–9.

83. Sezer İ. A Review Study on the Using of Diethyl Ether in Diesel Engines: Effects on Fuel Properties and Engine Performance. Energy Technology. 2018;6(11):2084–114.

84. Tree DR, Cooley WB. A Comparison and Model of NO x Formation for Diesel Fuel and Diethyl Ether. SAE Transactions. 2001;110:522–32.

85. Wang Y, Cao Y, Wei W, Davidson DF, Hanson RK. A new method of estimating derived cetane number for hydrocarbon fuels. Fuel. 2019 Apr 1;241:319–26.

86. Lequien G, Skeen S, Manin J, Pickett LM, Andersson O. Ignition Quality Effects on Lift-Off Stabilization of Synthetic Fuels. SAE International Journal of Engines. 2015;8(2):625–34.

87. ChemicalBook---Chemical Search Engine [Internet]. [cited 2021 Sep 28]. Available from: https://www.chemicalbook.com/productindex_en.aspx

88. Merck | France [Internet]. [cited 2021 Sep 28]. Available from: https://www.sigmaaldrich.com/FR/en

89. appendix-b.1,4-Dioxane Identifiers and the Physical and Chemical Properties of 1,4-Dioxanepdf [Internet]. [cited 2021 Sep 28]. Available from: https://14d-1.itrcweb.org/appendix-b/?print=pdf

90. Mzé-Ahmed A, Hadj-Ali K, Diévart P, Dagaut P. Kinetics of Oxidation of a Reformulated Jet Fuel (1-Hexanol/Jet A-1) in a Jet-Stirred Reactor: Experimental and Modeling Study. Combustion Science and Technology. 2012 Jul 1;184(7–8):1039–50.

91. Méthode de Joback. In: Wikipédia [Internet]. 2020 [cited 2021 Sep 28]. Available from: https://fr.wikipedia.org/w/index.php?title=M%C3%A9thode_de_Joback&oldid=177735137

92. ChemSpider | Search and share chemistry [Internet]. [cited 2021 Sep 28]. Available from: http://www.chemspider.com/

93. Guidechem 2-Penten-1-ol,2-methyl- [Internet]. [cited 2021 Sep 28]. Available from: https://www.guidechem.com/encyclopedia/2-penten-1-ol-2-methyl--dic123121.html

94. Aghbashlo M, Peng W, Tabatabaei M, Kalogirou SA, Soltanian S, Hosseinzadeh-Bandbafha H, et al. Machine learning technology in biodiesel research: A review. Progress in Energy and Combustion Science. 2021 Jul 1;85:100904.

95. Pöttering H-G, Necas P. Directive 2009/30/Ec of the European Parliament and of the Council of 23 April 2009. In: Core Statutes on Company Law [Internet]. London: Macmillan Education UK; 2015 [cited 2021 Sep 30]. p. 757–9. Available from: https://eur-lex.europa.eu/legal-content/EN/TXT/PDF/?uri=CELEX:32009L0030&from=EN

96. He, Y. Z., Mallard, W. G., Tsang, W., 1988. Kinetics of hydrogen and hydroxyl radical attack on phenol at high temperatures. The Journal of Physical Chemistry, 92(8), 2196–2201. doi:10.1021/j100319a023

97. Lovell, A.B., Brezinsky, K., Glassman, I., 1989. The gas phase pyrolysis of phenol. Int. J. Chem. Kinet. 21, 547–560. doi:10.1002/kin.550210706

98. Manion, J.A., Louw, R., 1989. Rates, products, and mechanisms in the gas-phase hydrogenolysis of phenol between 922 and 1175 K. J. Phys. Chem. 93, 3563–3574. doi:10.1021/j100346a040

99. Horn, C., Roy, K., Frank, P., Just, T., 1998. Shock-tube study on the high-temperature pyrolysis of phenol. Symposium (International) on Combustion 27, 321–328. doi:10.1016/S0082- 0784(98)80419-0

100. Brezinsky, K.; Pecullan, M.; Glassman, I. (1998). Pyrolysis and Oxidation of Phenol. The Journal of Physical Chemistry A, 102(44), 8614–8619. doi:10.1021/jp982177+

101. Mulcahy, M., Tucker, B., Williams, D., & Wilmshurst, J., 1967. Reactions of free radicals with aromatic compounds in the gaseous phase. III. Kinetics of the reaction of methyl radicals with anisole (methoxybenzene). Australian Journal of Chemistry, 20(6), 1155. doi:10.1071/ch9671155

102. Schlosberg, R., Szajowski, P., Dupre, G., Danik, J., Kurs, A., Ashe, T., Olmstead, W., 1983. Pyrolysis Studies of Organic Oxygenates .3. High-Temperature Rearrangement of Aryl Alkyl Ethers. Fuel 62, 690–694. **doi:10.1016/0016-2361(83)90308-3**

103. Lin, C.-Y., Lin, M.C., 1986. Thermal decomposition of methyl phenyl ether in shock waves: the kinetics of phenoxy radical reactions. J. Phys. Chem. 90, 425–431. **doi:10.1021/j100275a014**

104. Mackie, J.C., Colket, M.B., Nelson, P.F., 1990. Shock tube pyrolysis of pyridine. J. Phys. Chem. 94 4099–4106**. doi:10.1021/j100373a040**

105. Platonov, V.V., Proskuryakov, V.A., Ryl'tsova, S.V., Popova, Y.N., 2001. Homogeneous Pyrolysis of Anisole. Russian Journal of Applied Chemistry 74, 1047–1052. **doi:10.1023/A:1013076330586.**

106. Arends, Isabel W. C. E.; Louw, Robert; Mulder, Peter (1993). Kinetic study of the thermolysis of anisole in a hydrogen atmosphere. The Journal of Physical Chemistry, 97(30), 7914–7925. doi:10.1021/j100132a020

107. Friderichsen, A. V., Shin, E.-J., Evans, R. J., Nimlos, M. R., Dayton, D. C., & Ellison, G. B., 2001. The pyrolysis of anisole ($C_6H_5OCH_3$) using a hyperthermal nozzle. Fuel, 80(12), 1747–1755. **doi:10.1016/s0016-2361(01)00059-x.**

108. Pelucchia, M., Faravellia, T., Frassoldatia, A., Ranzia, E., SriBala, G., Marin Van, Guy B., Geem, K. Experimental and Kinetic Modeling Study of Pyrolysis and Combustion of Anisole. The Italian Association of Chemical Engineering. VOL. 65, 2018. **doi:10.3303/CET1865022**

109. Pecullan, M., Brezinsky, K., Glassman, I., 1997. Pyrolysis and Oxidation of Anisole near 1000 K. J. Phys. Chem. A 101, 3305–3316. **doi:10.1021/jp963203b**

110. Nowakowska, M., Herbinet, O., Dufour, A., Glaude, P.-A., 2014. Detailed kinetic study of anisole pyrolysis and oxidation to understand tar formation during biomass combustion and gasification. Combustion and Flame 161, 1474–1488. **doi: 10.1016/j.combustflame.2013.11.024**

111. Wu, Yi; Rossow, Bjorn; Modica, Vincent; Yu, Xilong; Wu, Linlin; Grisch, Frédéric (2017). Laminar flame speed of lignocellulosic biomass-derived oxygenates and blends of gasoline/oxygenates. Fuel, 202(), 572–582. **doi: 10.1016/j.fuel.2017.04.085**

112. Zare, Saeid; Roy, Shrabanti; El Maadi, Aiman; Askari, Omid (2019). An investigation on laminar burning speed and flame structure of anisole-air mixture. Fuel, 244(), 120–131. **doi: 10.1016/j.fuel.2019.01.149**

113. Bierkandt, Thomas; Hemberger, Patrick; Oßwald, Patrick; Krüger, Dominik; Köhler, Markus; Kasper, Tina (2018). Flame structure of laminar premixed anisole flames investigated by photoionization mass spectrometry and photoelectron spectroscopy. Proceedings of the Combustion Institute, (), S1540748918304553**–. doi: 10.1016/j.proci.2018.07.037**

114. Zhou, Lei; Yu, Dan; Wang, Zhen; Cheng, Li-Juan; Jin, Zhi-Hao; Weng, Jun-Jie; Yang, Jiu-Zhong; Tian, Zhen-Yu (2019). A detailed kinetic study on oxidation of benzyl alcohol. Combustion and Flame, 207(), 10–19. doi: 10.1016/j.combustflame.2019.05.034

115. Taylor, Roger (1988). The mechanism of thermal eliminations. Part 25. Arrhenius data for pyrolysis of isochroman-3-one, benzyl methyl ether, 2-hydroxyethylbenzene, phenyl acetate, and 3,4-dihydro-2H-pyran. Journal of the Chemical Society, Perkin Transactions 2, (2), 183–. doi:10.1039/p29880000183

116. Gabriel Chuchani; Alexandra Rotinov; Rosa M. Dominguez (1999). The kinetics and mechanisms of gas phase elimination of primary, secondary, and tertiary 2-hydroxyalkylbenzenes. 31(6), 401–407. **doi:10.1002/(sici)1097-4601(1999)31:6<401: aid-kin1>3.0.co;2-z**

117. Etz, Brian D.; Fioroni, Gina M.; Messerly, Richard A.; Rahimi, Mohammad J.; St. John, Peter C.; Robichaud, David J.; Christensen, Earl D.; Beekley, Brian P.; McEnally, Charles S.; Pfefferle, Lisa D.; Xuan, Yuan; Vyas, Shubham; Paton, Robert S.; McCormick, Robert L.; Kim, Seonah (2020). Elucidating the chemical pathways responsible for the sooting tendency of 1 and 2-phenylethanol. Proceedings of the Combustion Institute, (), S1540748920301279–. doi: 10.1016/j.proci.2020.06.072

118. Ben-Dor, Gabi; Sadot, Oren; Igra, Ozer (2017). 30th International Symposium on Shock Waves 1 || Shock Tube Experimental and Theoretical Study on the Thermal Decomposition of 2-Phenylethanol. , 10.1007/978-3-319-46213-4(Chapter 53), 317–320. **doi:10.1007/978-3-319-46213-4_53**

119. Shankar, Vijai Shankar Bhavani; Al-Abbad, Mohammed; El-Rachidi, Mariam; Mohamed, Samah Y.; Singh, Eshan; Wang, Zhandong; Farooq, Aamir; Sarathy, S. Mani (2016). Antiknock quality and ignition kinetics of 2-phenylethanol, a novel lignocellulosic octane booster. Proceedings of the Combustion Institute, (), S1540748916300414–. **doi: 10.1016/j.proci.2016.05.041**

120. Ruozhou, Fang., Chih-Jen Sung., 2021. A Rapid Compression Machine Study of 2-Phenylethanol Autoignition at Low-To-Intermediate Temperatures. Energies 2021, 14, 7708. **https://doi.org/10.3390/en14227708**

121. Wornat, M. J., Ledesma, E. B., Marsh, N. D., 2001. Polycyclic aromatic hydrocarbons from the pyrolysis of catechol (ortho-dihydroxybenzene), a model fuel representative of entities in tobacco, coal, and lignin. Fuel, 80(12), 1711–1726. **doi:10.1016/s0016-2361(01)00057-6**

122. Ledesma, E. B., Marsh, N. D., Sandrowitz, A. K., Wornat, M. J., 2002. An experimental study on the thermal decomposition of catechol. Proceedings of the Combustion Institute, 29(2), 2299–2306. **doi:10.1016/s1540-7489(02)80280-2**

123. Thomas, S., Ledesma, E. B., Wornat, M. J., 2007. The effects of oxygen on the yields of the thermal decomposition products of catechol under pyrolysis and fuel-rich oxidation conditions. Fuel, 86(16), 2581–2595. **Doi : 10.1016/j.fuel.2007.02.003**

124. Martino, Christopher J.; Savage, Phillip E.; Kasiborski, John (1995). Kinetics and Products from o-Cresol Oxidation in Supercritical Water. Industrial & Engineering Chemistry Research, 34(6), 1941–1951. doi:10.1021/ie00045a003

125. Martino, Christopher J.; Savage, Phillip E. (1997). Thermal Decomposition of Substituted Phenols in Supercritical Water. Industrial & Engineering Chemistry Research, 36(5), 1385–1390. **doi:10.1021/ie960698i**

126. Klein, M. T., Virk, P. S., 1980. Model Pathways for Gas Release from Lignites. Prepr. Pap. -Am. Chem. Soc., Div. Fuel Chem. 25, 180.

127. Ceylan, R., Bredenberg, J. B., 1982. Hydrogenolysis and Hydrocracking of the Carbon-Oxygen Bond. 2. Thermal Cleavage of the Carbon-Oxygen Bond in Guaiacol. Fuel 1982, 61, 377–382. **doi :10.1016/0016-2361(82)90054-0**

128. Scheer, A. M., Mukarakate, C., Robichaud, D. J., Nimlos, M. R., Ellison, G. B., 2011. Thermal Decomposition Mechanisms of the Methoxyphenols: Formation of Phenol, Cyclopentadienone, Vinylacetylene, and Acetylene. The Journal of Physical Chemistry A, 115 (46), 13381–13389. **doi:10.1021/jp2068073**

129. Nowakowska, M., Herbinet, O., Dufour, A., Glaude, P.-A., 2018. Kinetic Study of the Pyrolysis and Oxidation of Guaiacol. The Journal of Physical Chemistry A. **doi: 10.1021/acs.jpca.8b06301**